Table 3. Primer-probe sets for real-time RT-PCR experiments used in experimental tuberculosis of guinea pig

Target	Sequence (5'-3')[a] (S: sense, A: antisense, P: probe)	Length of Amplicon (bp)
GAPDH	S: CGG ATT TGG CCG TAT TGG A: AAT ATC CAC TTT GCC AGA CAT GAA P: FAM-CGC CTG GTC ACC AGG GCT GC-TAMRA	64
IFN-γ	S: ACA AGG TGC AGG CTT TCA AAA A: TTG GCG CTG GAC ATG CT P: FAM-CCT GAT TCA AAT TTC GGT CAA TGA-TAMRA	65
TNF-α	S: TGG CCC CCC CTT CAG A A: TGT CAT TAT CGT TTT GAG AAG CTG AT P: FAM-CTG GCC CAG ACG CTC ACA CTC A-TAMRA	68
iNOS	S: GCA GCA GCG GCT TCA CA A: ACA TCC AAA CAG GAG CGT CAT T P: FAM-CTC AAA CAC ACA GGG CTC CAG GGT G-TAMRA	70

a: Primers and probes were designed by Primer Express software (version 2.0.0; Applied Biosystems). FAM and TAMRA were used as reporter and quencher fluorescent dyes, respectively.

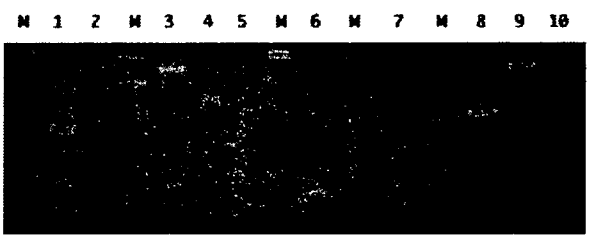

Fig. 1. Results of RT-PCR of β-actin, GAPDH, IFN-γ, TNF-α and iNOS. Lane 1: β-actin PCR products (279 bp) amplified from cDNA from guinea pig lung tissue sample using the primer sets designed by Nishikawa *et al.* [13]; lane 3: GAPDH PCR product amplified from cDNA from a guinea pig lung tissue sample with CLONTEC primer set (452 bp); lane 4: GAPDH PCR products amplified from cDNA from guinea pig lung tissue sample with CLONTEC sense primer and Primer 3-designed anti-sense primer (343 bp). Lane 6: IFN-γ PCR products amplified from cDNA from a guinea pig lung tissue sample with the Primer 3-designed primer set (171 bp); lane 7: TNF-α PCR products amplified from cDNA from a guinea pig lung tissue sample with the Primer 3-designed primer set (184 bp); lane 8: reference PCR product (317 bp) using cDNA from a rat lung tissue and the rat primer set for iNOS; lane 9; iNOS PCR products amplified from cDNA from a guinea pig lung tissue sample with the primer set designed by reference to the rat iNOS primer set (456 bp). Lanes 2 and 5: negative control PCR products using β-actin and GAPDH primer sets, respectively; lane 10: an example of negative control PCR products with iNOS primer sets. In negative control experiments, purified and non-reverse transcribed mRNA samples were used for PCR. M: molecular size marker.

signed by CLONTEC Laboratories, Inc., which are used to detect human, mouse and rat GAPDH of the same product length. The length of the guinea pig PCR product thus obtained was also the same (452 bp). The PCR product shown in lane 4 was amplified using a newly designed antisense primer specific for guinea pig GAPDH (Table 2). The product length obtained with this primer set was 343 bp. The signal for the latter product was slightly lower than that for the former under the same PCR conditions. It was shown that no DNA contamination occurred in the purified mRNA used as template because there was no product after PCR (lanes 2 and 5).

Primer sets for IFN-γ, TNF-α and iNOS

Figure 1 also shows the PCR data for IFN-γ, TNF-α and iNOS mRNA expression. Although attempts were made to design specific primer sets for guinea pig IFN-γ and TNF-α using the sequence information (homology or complementarity) for mice and rats, it proved impossible to design satisfactory primer sets. Therefore, primer sets for IFN-γ and TNF-α were designed using the primer design program, Primer 3. With these primer sets, clear PCR product bands of 171 bp (IFN-γ, lane 6) and 184 bp (TNF-α; lane 7), were obtained. Primer sets for iNOS were designed based on sequence homology to the rat iNOS gene as shown in Table 2. With these primer sets, clear PCR bands of 456 bp were

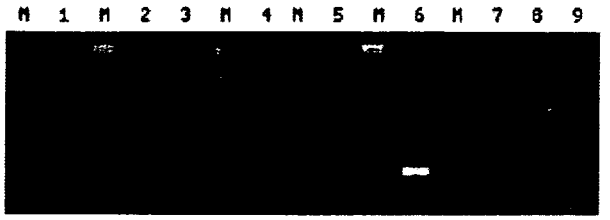

Fig. 2. Results of RT-PCR of IL-1β, IL-2, IL-10, IL-12p40, GM-CSF, and TGF-β. Lane 1: IL-1β PCR products amplified from cDNA from a guinea pig lung tissue sample with a primer set designed by Primer 3 software (430 bp); lane 2: reference IL-2 PCR product (401 bp) amplified using mouse lung cDNA and the mouse primer set; lane 3: IL-2 PCR products amplified from cDNA from a guinea pig lung tissue sample with a primer set designed by reference to the mouse IL-2 primer set (353 bp); lane 4: IL-10 PCR products amplified from cDNA from a guinea pig lung tissue sample with a Primer 3-designed primer set (367 bp); lane 5: IL-12 p40 PCR products amplified with a Primer 3-designed primer set (296 bp); lane 6: GM-CSF PCR products amplified from cDNA from a guinea pig lung tissue sample with a Primer 3-designed primer set (171 bp); lane 7: reference PCR product of TGF-β PCR product amplified from cDNA from a mouse lung tissue sample with the mouse primer set (405 bp); lane 8: TGF-β PCR products amplified from cDNA from a guinea pig lung tissue sample with a primer set designed by referring to the mouse TGF-β primer set (303 bp); lane 9: an example of negative control PCR products with TGF-β primer set, where purified and non-reverse transcribed mRNA samples were used for PCR. M: molecular size marker.

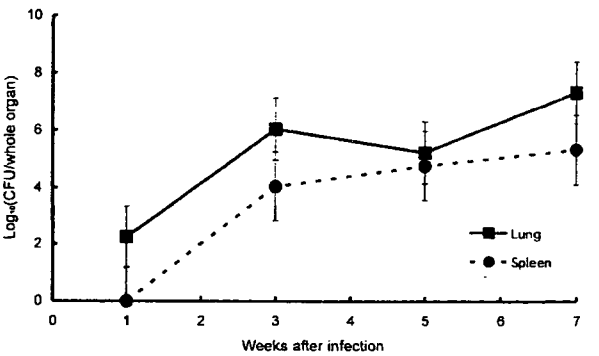

Fig. 3. CFU changes in lung and spleen tissue of *M. tuberculosis*-infected guinea pigs. Animals were sacrificed at the indicated time points, tissue homogenates were plated on Ogawa's media, and the number of colonies was counted after four weeks of culture at 37°C. The results were expressed as means of triplicate experiments.

obtained for guinea pigs (lane 9) and 317 bp for rats (lane 8) with corresponding primer sets, respectively.

Figure 2 shows the data for RT-PCR using six primer sets designed for guinea pig IL-1β, IL-2, IL-10, IL-12 p40, GM-CSF and TGF-β mRNA. Among these, the primer sets for IL-2 were constructed using homology with mouse primer sequences that we use in our laboratory and a PCR product with an expected length of 353 bp (lane 3) was obtained. The reference PCR product for IL-2 (401 bp) obtained with combination of a mouse cDNA template and primers for mouse IL-2 is also shown in lane 2. As it was difficult to design satisfactory gene primer sets for IL-1β, IL-10 and IL-12 p40 from mouse or rat RT-PCR primer sets, the Primer 3 program was used (Table 2) and products of 430 bp (IL-1β; lane 1), 367 bp (IL-10; lane 4) and 296 bp (IL-12 p40; lane 5) were obtained.

Finally, guinea pig primer sets for TGF-β and GM-CSF were designed. The primer set for guinea pig TGF-β was designed by referring to the mouse primer set for TGF-β (Table 2). A clear 303-bp PCR product was observed (lane 8) for guinea pig samples with guinea pig primer sets. The reference PCR products (405 bp) with mouse cDNA samples and mouse primer sets are shown in lane 7. The primer set for GM-CSF was designed using the Primer 3 program, and the PCR product was shown to be 171 bp in length (lane 6).

Comparison of the results of RT-PCR with those of real-time RT-PCR

We performed real-time RT-PCR for some of the important target genes to compare the results with those of conventional RT-PCR. The guinea pigs were infected by the aerosol technique with the Kurono strain of *M. tuberculosis*, and sacrificed at two-week intervals from 1 week post-infection. The numbers of CFU in the infected lung and spleen tissues were determined by culturing the tissue homogenates for 4 weeks at 37°C (Fig. 3). The number of tubercle bacilli in lung and spleen tissues increased gradually with time except at five weeks post-infection in the lung tissues. There were no tubercle bacilli at one week post-infection in the spleen, but the number increased gradually thereafter.

In view of the importance of cytokines in *M. tuberculosis* infection, IFN-γ, TNF-α, and iNOS were chosen as target genes and the primer-probe sets for these target genes were synthesized. The primer-probe set for GAPDH was also synthesized and used as an internal

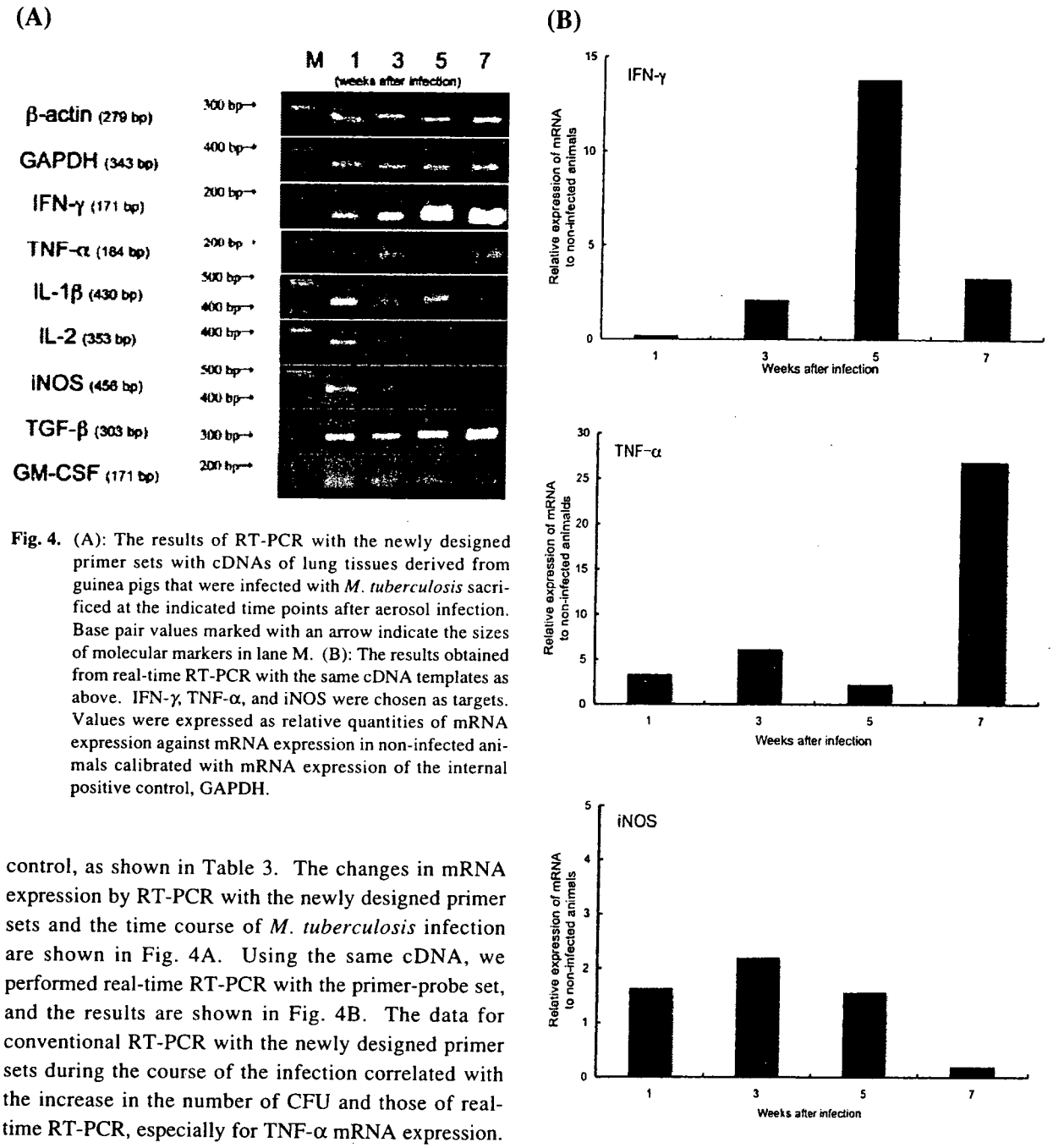

Fig. 4. (A): The results of RT-PCR with the newly designed primer sets with cDNAs of lung tissues derived from guinea pigs that were infected with *M. tuberculosis* sacrificed at the indicated time points after aerosol infection. Base pair values marked with an arrow indicate the sizes of molecular markers in lane M. (B): The results obtained from real-time RT-PCR with the same cDNA templates as above. IFN-γ, TNF-α, and iNOS were chosen as targets. Values were expressed as relative quantities of mRNA expression against mRNA expression in non-infected animals calibrated with mRNA expression of the internal positive control, GAPDH.

control, as shown in Table 3. The changes in mRNA expression by RT-PCR with the newly designed primer sets and the time course of *M. tuberculosis* infection are shown in Fig. 4A. Using the same cDNA, we performed real-time RT-PCR with the primer-probe set, and the results are shown in Fig. 4B. The data for conventional RT-PCR with the newly designed primer sets during the course of the infection correlated with the increase in the number of CFU and those of real-time RT-PCR, especially for TNF-α mRNA expression.

Discussion

The guinea pig model is one of the most suitable animal models for simulating human TB [11]. There have been many experimental studies using guinea pigs to assess the efficacy of newly produced vaccines and antibiotics [3–5, 7, 24]. However, as there are very few useful tools for evaluating the immunological changes in these experiments at the protein and genetic levels, some researchers have used bioassays to measure IFN-γ or northern blot hybridization using limited numbers of DNA probes [2, 6]. Antibodies against guinea pig cytokines are not available for setting up guinea pig cytokine ELISA. So far, guinea pig IFN-γ,

TNF-α, IL-1β, IL-2, IL-10, IL-12p40, GM-CSF, TGF-β and iNOS mRNA have been sequenced and their accession numbers are readily available [7, 15, 20], but RT-PCR has not been available for examining the expression of these mRNAs. Thus, our study is useful because our RT-PCR detects immunological changes in *M. tuberculosis*-infected guinea pig tissues at the mRNA level over time. Recently, a highly quantitative mRNA detection system, real-time PCR, has been introduced to the field of TB investigation [1, 2, 8, 10]. Although this technique provides quantitative results, the reagents are expensive and special devices are required. Thus, we designed primer sets for conventional reverse transcription PCR that can be used with cheaper reagents and simpler devices.

When we designed the primer sets for guinea pig cytokines and iNOS, we adopted two methods. First, we searched for homology in cytokine genes among guinea pig, mouse and rat with information obtained from the DDBJ and the National Center for Biochemical Information (NCBI). This enabled us to design two cytokine primer sets for guinea pig genes, IL-2 and TGF-β, and a primer set for iNOS. As shown in Table 1, primer sets for IL-2 and TGF-β, and iNOS were designed utilizing mRNA sequence homology to the corresponding genes of the mouse and the rat. Secondly, we used Primer 3 (an on-line primer design program) to design primer sets. This program provides an easy method for preparing primer sets using default settings. We prepared new primer sets for guinea pig IFN-γ, TNF-α, IL-1β, IL-10, IL-12p40, and GM-CSF using this program.

There is only very limited information available about the guinea pig genomic sequence, therefore, we do not know if there are any exon-intron boundaries in the regions targeted for PCR amplification. We have to purify mRNAs from guinea pig tissues in order to prevent genomic DNA contamination, otherwise it is difficult to know whether the resultant PCR products have been amplified only from reverse-transcribed cDNA. In this study, we used an Oligo dT-30 <Super> mRNA purification kit (Takara-Bio, Co. Ltd., Shiga, Japan) to purify mRNA from total RNA extracted from the guinea pig tissues. This kit utilizes the presence of the poly A tail of the mRNA sequence and provided excellent mRNA purification with no genomic DNA contamination. This mRNA purification method is very useful when PCR is performed using guinea pig mRNA samples for which the information about exon-intron boundaries is unknown. This step is essential and other mRNA purification kits can be used.

We have already reported several mRNA expression patterns with RT-PCR for cytokines and other effector molecules in experimental tuberculosis with mouse and rat models [16–19, 22, 23]. In these reports, wild type animals expressed TNF-α mRNA from early days after infection, and mRNA expression pattern of iNOS correlated very well with that of IFN-γ, where both peaks of expression appeared at 3 to 5 weeks after infection. Up-regulated expression of these cytokines and iNOS in the early period of infection is important to prevent deterioration of the disease.

In this study, we investigated mRNA expression patterns of several cytokines and iNOS in experimental tuberculosis of the guinea pig with conventional RT-PCR and real-time PCR (for IFN-γ, TNF-α and iNOS). In terms of TNF-α, the expression pattern in guinea pig was similar to those of the mouse and rat which we have reported several times [16–19, 22, 23], and the results from RT-PCR and real-time PCR correlated very well with each other. However, although the mRNA expression pattern of IFN-γ examined by RT-PCR was similar to those of the mouse or rat, the expression pattern of iNOS did not correlate well with IFN-γ despite repeated trials. It is thought that this phenomenon is typical of the guinea pig. The results of RT-PCR showed slight differences with the expression patterns examined with real-time PCR. Recently, Raju *et al.* reported there was no correlation between IFN-γ and iNOS expression in an examination of BAL cells with real-time PCR when tuberculosis patients were treated with aerosolized IFN-γ, whereas the IFN-γ inducible 10-kDa protein (IP-10) expression examined with real-time PCR correlated well with the administered dose of IFN-γ [14]. Our present data are in agreement with their evidence and both may reflect an immunological similarity between the human and guinea pig in co-expression patterns of IFN-γ and iNOS

We also assessed whether or not the primer sets could provide satisfactory outcomes in tissues of *M. tuberculosis*-infected guinea pigs, and compared the data with those of real-time RT-PCR. The data obtained using both methods were correlated. The correlation indicates that the newly designed primer sets for

conventional RT-PCR can serve as useful immunological tools in guinea pig experiments. Using these primer sets, conventional RT-PCR in the guinea pig can provide valuable data more conveniently and cheaper than real-time PCR.

In summary, we devised new primer sets for guinea pig gene RT-PCR, and they will be useful for immunological studies of TB in guinea pigs. RT-PCR is a convenient and cost-effective method although it is semi-quantitative. Few tools are currently available for examining the immunological processes in guinea pig TB, therefore, these newly designed primer sets for RT-PCR will serve as effective and less expensive experimental tools that can be used routinely for research in this field.

References

1. Allen, S.S. and McMurray, D.N. 2003. Coordinate cytokine gene expression in vivo following induction of tuberculosis pleurisy in guinea pigs. *Infect. Immun.* 71: 4271–4277.
2. Allen, S.S., Cassone, L., Lasco, T.M., and McMurray, D.N. 2004. Effect of neutralizing transforming growth factor β1 on the immune response against *Mycobacterium tuberculosis* in guinea pigs. *Infect. Immun.* 72: 1358–1363.
3. Aubry, A., Pan, X.S., Fisher, L.M., Jarlier, V., and Cambau, E. 2004. *Mycobacterium tuberculosis* DNA gyrase: interaction with quinolones and correlation with antimycobacterial drug activity. *Antimicrob. Agents Chemother.* 48: 1281–1288.
4. Dascher, C.C., Hiromatsu, K., Xiong, X., Morehouse, C., Watts, G., Liu, G., McMurray, D.N., LeClair, K.P., Porcelli, S.A., and Brenner, M.B. 2003. Immunization with a mycobacterial lipid vaccine improves pulmonary pathology in the guinea pig model of tuberculosis. *Int. Immunol.* 15: 915–925
5. Horwitz, M.A. and Harth, G. 2003. A new vaccine against tuberculosis affords greater survival after challenge than the current vaccine in the guinea pig model of pulmonary tuberculosis. *Infect. Immun.* 71: 1672–1679.
6. Jeevan, A., Yoshimura, T., Foster, G., and McMurray, D.N. 2002. Effect of *Mycobacterium bovis* BCG vaccination on interleukin-1β and RANTES mRNA expression in guinea pig cells exposed to attenuated and virulent mycobacteria. *Infect. Immun.* 70: 1245–1253.
7. Jeevan, A., Yoshimura, T., Lee, K.E., and McMurray, D.N. 2003. Differential expression of gamma interferon mRNA induced by attenuated and virulent *Mycobacterium tuberculosis* in guinea pig cells after *Mycobacterium bovis* BCG vaccination. *Infect. Immun.* 71: 354–364.
8. Kawahara, M., Nakasone, T., and Honda, M. 2002. Dynamics of gamma interferon, interleukin-12 (IL-12), IL-10, and transforming growth factor beta mRNA expression in primary *Mycobacterium bovis* BCG infection in guinea pigs measured by a real-time fluorogenic reverse transcription-PCR assay. *Infect. Immun.* 70: 6614–6620.
9. Lasco, T.M., Yamamoto, T., Yoshimura, T., Allen, S.S., Cassone, L., and McMurray, D.N. 2003. Effect of *Mycobacterium bovis* BCG vaccination on *Mycobacterium*-specific cellular proliferation and tumor necrosis factor alpha production from distinct guinea pig leukocyte populations. *Infect. Immun.* 71: 7035–7042.
10. Lyons, M.J., Yoshimura, T., and McMurray, D.N. 2002. *Mycobacterium bovis* BCG vaccination augments interleukin-8 mRNA expression and protein production in guinea pig alveolar macrophages infected with *Mycobacterium tuberculosis*. *Infect. Immun.* 70: 5471–5478.
11. McMurray, D.N. 1994. Guinea pig model of tuberculosis. In Tuberculosis. Pathogenesis, protection, and control. Ed. by Bloom, B. R. ASM Press, Washington, D.C.
12. Morishima, Y., Nomura, A., Uchida, Y., Noguchi, Y., Sakamoto, T., Ishii, Y., Goto, Y., Masuyama, K., Zhang, M. J., Hirano, K., Mochizuki, M., Ohtsuka, M., and Sekizawa, K. 2001. Triggering the induction of myofibroblast and fibrogenesis by airway epithelial shedding. *Am. J. Respir. Cell Mol. Biol.* 24: 1–11.
13. Nishikawa, M., Kakemizu, N., Ito, T., Kudo, M., Kaneko, T., Suzuki, M., Udaka, N., Ikeda, H., and Okubo, T. 1999. Superoxide mediates cigarette smoke-induced infiltration of neutrophils into the airways through nuclear factor-κB activation and IL-8 mRNA expression in guinea pigs *in vivo*. *Am. J. Respir. Cell Mol. Biol.* 20: 189–198.
14. Raju, B., Hoshino, Y., Kuwabara, K., Belitskaya, I., Prabhakar, S., Canova, A., Gold, J.A., Condos, R., Pine, R.I., Brown, S., Rom, W.N., and Weiden, M.D. 2004. Aerosolized gamma interferon (IFN-gamma) induces expression of the genes encoding the IFN-gamma-inducible 10-kilodalton protein but not inducible nitric oxide synthase in the lung during tuberculosis. *Infect. Immun.* 72: 1275–1283.
15. Shirato, M., Sakamoto, M., Uchida, Y., Nomura, A., Ishii, Y., Iijima, H., Goto, Y., and Hasegawa, S. 1998. Molecular cloning and characterization of Ca^{2+}-dependent inducible nitric oxide synthase from guinea pig lung. *Biochem. J.* 333: 795–799.
16. Sugawara, I., Mizuno, S., Yamada, H., Matsumoto, M., and Akira, S. 2001. Disruption of nuclear factor-interleukin-6 (NF-IL6), a transcription factor, results in severe mycobacterial infection. *Am. J. Pathol.* 158: 361–366.
17. Sugawara, I., Yamada, H., Mizuno, S., Li, C.Y., Nakayama, T., and Taniguchi, M. 2002. Mycobacterial infection in natural killer T cell knockout mice. *Tuberculosis* 82: 97–104.
18. Sugawara, I., Yamada, H., and Mizuno, S. 2004. Pulmonary tuberculosis in spontaneously diabetic goto kakizaki rats. *Tohoku J. Exp. Med.* 204: 135–145.
19. Sugawara, I., Yamada, H., and Mizuno, S. 2004. Pathological and immunological profiles of rat tuberculosis. *Int. J. Exp. Pathol.* 85:125–134.
20. Wicher, V., Scarozza, A.M., Ramsingh, A.I., and Wicher, K. 1998. Cytokine gene expression in skin of susceptible guinea pig infected with *Treponema pallidum*. *Immunology*

95: 242–247.
21. World Health Organization. 2003. WHO Report 2003. Global tuberculosis control. [Online] www.who.int/gtb/publications/globrep/index.html.
22. Yamada, H., Mizuno, S., Horai, R., Iwakura, Y., and Sugawara, I. 2000. Protective role of interleukin-1 in mycobacterial infection in IL-1 α/β double knockout mice. *Lab. Invest.* 80: 759–767.
23. Yamada, H., Mizuno, S., Reza-Gholizadeh, M., and Sugawara, I. 2001. Relative importance of NF-kappaB p50 in mycobacterial infection. *Infect. Immun.* 69: 7100–7105.
24. Yildirim, Z., Hacievliyagil, S., Kutlu, N.O., Aydin, N.E., Kurkcuoglu, M., Iraz, M., and Durmaz, R. 2004. Effect of water extract of Turkish propolis on tuberculosis infection in guinea pigs. *Pharmacol. Res.* 49: 287–292.

Cellular Microbiology (2006) 8(4), 661–667

doi:10.1111/j.1462-5822.2005.00658.x
First published online 28 November 2005

Nude rat (F344/N-rnu) tuberculosis

Isamu Sugawara,* Hiroyuki Yamada and Satoru Mizuno
Mycobacterial Reference Center, The Research Institute of Tuberculosis, Kiyose, Tokyo 204-0022, Japan.

Summary

As many mononuclear cells from *Mycobacterium tuberculosis*-infected lung tissues are not available for fluorescence-activated cell sorter (FACS) analysis and the tuberculin test is not feasible in a mouse tuberculosis model, we attempted to develop a rat tuberculosis model. We have previously reported that rat tuberculosis is associated with granulomas that lack central necrosis. In order to develop a better animal model of tuberculosis in immunocompromised humans (tuberculosis associated with HIV infection or tuberculosis of the elderly), we infected F344/N-rnu nude rats with *M. tuberculosis* via the airborne route. The animals developed pulmonary granulomas with central necrosis encapsulated by dense collagen fibres, closely resembling those of human tuberculosis. The nude rats died of disseminated tuberculosis by the 85th day after aerosol infection, while F344 wild-type rats did not. Interestingly, T-cells that were reactive with anti-CD4 antibody and anti-CD8 antibody, indicating the presence of remnant thymus, were observed in the infected lung tissues of the nude rats. Therefore, T-cell precursors may be present in nude rats. The nude rat tuberculosis model mimics tuberculosis in immunocompromised humans and may provide a suitable model for immunological studies *in vivo*.

Introduction

Mice and guinea pigs have been commonly used as animal models of human tuberculosis (McMurray, 1994; Orme and Collins, 1994). Mice show lower tuberculin sensitivity than humans, and exhibit no caseous necrosis. Guinea pigs, a species with good delayed-type hypersensitivity, are very susceptible and usually develop a blood-disseminated disease similar to that observed in infants and immunosuppressed individuals. Pulmonary granulomas can be induced reproducibly with *Mycobacterium tuberculosis*, *M. avium* and *M. bovis* in these animals (Francis, 1958; Dannenberg, 1999). However, guinea pigs are not suitable for immunological studies because there are few congenic strains and insufficient numbers of monoclonal antibodies (Abs) against guinea pigs are available for immunological analysis. Mice are frequently used for such purposes because many congenic strains are available and murine immunology, like human immunology, has been well studied. However, for investigating the roles of cells in *M. tuberculosis*-infected pulmonary tissue in more detail, the murine model is not suitable because it is difficult to obtain mononuclear cells for immunological analysis from murine lung tissue and to perform tuberculin tests intradermally because of the extreme thinness of murine skin. Recently, however, novel approaches (lung digestion to isolate lung cells, *in situ* studies of cytokine production using immunohistochemistry and laser capture microdissection) have been developed to overcome these difficulties (Aung *et al.*, 2000; Scott and Flynn, 2002; Selva *et al.*, 2004).

We have recently reported a rat tuberculosis model that can overcome the problems associated with the murine model, including the inapplicability of the tuberculin test and the relative paucity of pulmonary mononuclear cells for fluorescence-activated cell sorter (FACS) analysis (Sugawara *et al.*, 2004a). Tuberculous lesions were induced in rats by aerial infection. There are several advantages of using rats instead of mice. Rat immunology is relatively well documented and in this species it is relatively easy to collect mononuclear cells from infected lung tissue. Moreover, monoclonal Abs for examining the role of T-cells, natural killer (NK) cells, macrophages and even dendritic cells are commercially available. There have been no detailed studies on the pathogenesis of rat tuberculosis induced with *M. tuberculosis* via the airborne route, although there have been several reports on rat tuberculosis induced by intravenous injection of *M. tuberculosis*, *M. avium* and *M. bovis* (Wessels, 1941a,b; Francis, 1958). Diabetic Goto-Kakizaki rats are also useful for investigating the relationship between diabetes mellitus and tuberculosis. This close relationship has been mentioned in several papers (Banyai, 1931; Root, 1934; Boucot *et al.*, 1952). We have confirmed that there is a close association between experimental tuberculosis and diabetes in animals, and that alveolar macrophages from Goto-Kakizaki diabetic rats are not fully activated by *M. tuberculosis* infection (Sugawara *et al.*,

Received 15 August, 2005; revised 7 October, 2005; accepted 12 October, 2005. *For correspondence. E-mail sugawara@jata.or.jp; Tel. (+81) 424 93 5075; Fax (+81) 424 92 4600.

2004b). Although rat tuberculosis is useful for immunological research, the granulomas are histologically similar to murine granulomas in lacking central necrosis. This discrepancy in histopathology between rat and human tuberculosis prompted us to explore another rat tuberculosis model. Here we describe a model of tuberculosis in the F344/N-rnu nude rat strain, which is derived from the Rowett nude rat strain established in 1953 (Kuramoto *et al.*, 1993). F344/N-rnu nude rats have remnant thymuses, and histologically they develop granulomas with central necrosis encapsulated by thick collagen fibres, thus resembling those in humans. This is the first description of the histopathological and immunological profiles of infected lung tissue in nude rat tuberculosis.

Results

Mycobacterial burden in the lungs and spleens of nude rats

All F344 rats survived the entire experimental period, but F344/N-rnu nude rats died of disseminated tuberculosis by the 85th day after infection (Fig. 1). The numbers of tubercle bacilli recovered from the lungs and spleen tissue of the infected animals after aerosol infection are shown as colony-forming units (cfu) in Fig. 2. One week after infection, tubercle bacilli were recovered only from the lung tissues. The mycobacterial load in the lungs had increased 3 weeks after infection, and gradually increased thereafter up to week 12. There was a statistically significant difference in pulmonary and splenic cfu at 6, 8 and 12 weeks after infection between F344 rats and F344/N-rnu nude rats ($P < 0.01$). No tubercle bacilli were recovered from spleens 1 week after infection. The mycobacterial load in the spleen tissue of F344/N-rnu nude rats continued to increase up to 12 weeks.

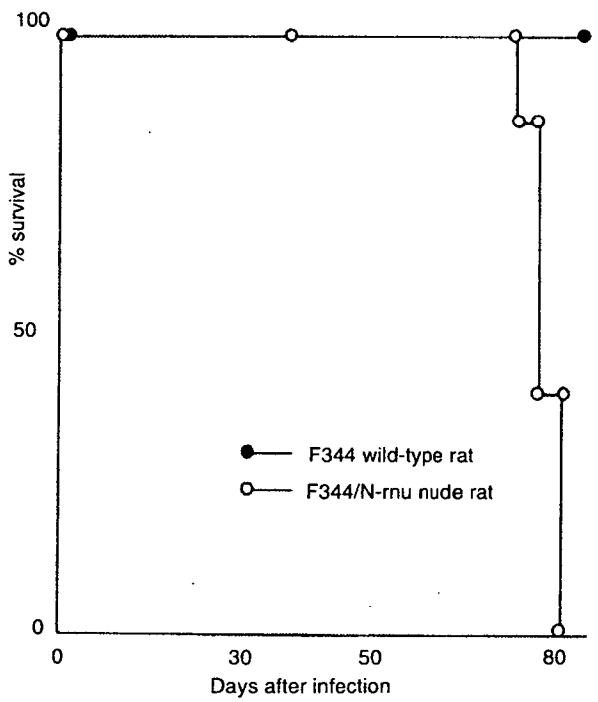

Fig. 1. Survival curves of F344/N-rnu nude rats infected with *M. tuberculosis* Kurono strain. The data presented are from two separate experiments with 10 rats in each group.

Light microscopic observation of infected lungs

Rats were sacrificed 1, 3, 6, 8 and 12 weeks after infection with *M. tuberculosis*, and formalin-fixed sections were stained with haematoxylin and eosin (HE) and by the Ziehl-Neelsen method (Sugawara *et al.*, 2004b). Non-specific non-granulomatous pneumonia was recognized in the lung tissue 1 week after infection, but from 3 weeks after infection multiple granulomas of various sizes showing central necrosis were seen in the lungs (Fig. 3A). Foamy macrophages began to appear in the granulomatous lesions 5 weeks after infection, were most conspicuous at 7 weeks, and were still recognizable in the lungs even at 12 weeks. Multinucleate giant cells were evident in the lungs 12 weeks after infection. Similar small granulomas were recognized in the spleen and liver. Figure 3E shows the representative histopathology of lungs removed from F344/N-rnu nude rats at 12 weeks after infection, numerous tubercle bacilli being recognizable in the granulomatous lesions. The granulomas consisted of lymphocytes, epithelioid macrophages and foamy macrophages (especially at 5 and 7 weeks after infection). At 12 weeks after infection, the granulomas were surrounded by thick collagen fibres, but still contained a number of tubercle bacilli. These pulmonary lesions were very similar to those of human pulmonary tuberculosis, but the central necrosis was not caseous (Fig. 3E). Granulomas of various sizes were recognized in the spleen, liver and lymph nodes, but these showed central necrosis. However, the granulomas of F344 wild-type rats lacked central necrosis (Fig. 3B, D and F).

Fluorescence-activated cell sorter (FACS) analysis

The baseline control data for anti-CD4 monoclonal Ab, anti-CD8 monoclonal Ab, anti-NK cell monoclonal Ab, OX52, OX62, ED1, anti-rat α/βT-cell monoclonal Ab, and anti-rat γ/δT-cell monoclonal Ab in uninfected rat pulmonary tissues were close to zero by FACS analysis. The temporal expression of antigens recognized by these Abs was then followed up by FACS (Fig. 4A and B). ED1 antigen was expressed at a significantly high level 1 week after infection and this expression was maintained up to 12 weeks, there being no significant differ-

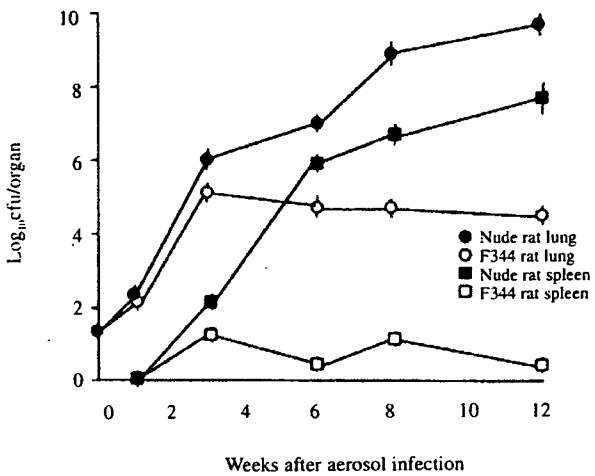

Fig. 2. Colony-forming unites (cfu) in lung and spleen tissues of F344/N-rnu nude and wild-type rats (15 rats each) infected with the Kurono strain by the airborne route. At the indicated weeks after infection, three rats from each group were sacrificed and homogenates of lung and spleen tissues were plated. Upon delivery at day 1, cfu per lung was 110 ± 10. Error bars indicate standard errors of the means.

ence in expression between F344 and F344/N-rnu nude rats. OX62 antigen was expressed weakly at 1 week after infection, but by 3, 6 and 8 weeks after infection, its expression had increased almost 10-fold. At 3 weeks after infection, there was a significant difference in the number of pulmonary OX62-positive cells between F344 and F344/N-rnu nude rats ($P < 0.01$). OX52 antigen (equivalent to CD6) expression was less than 20% at 1 week after infection and remained at the same level throughout the observation period. The total number of T-cells expressing OX52 was a little higher than that of T-cells expressing CD4 and CD8. CD4 antigen expression was low 1 week after infection and remained at the same level throughout the observation period. Anti-CD4 monoclonal Ab (Serotec) was reactive with immature T-cells. On the other hand, at 1 week after infection, expression of CD8 antigen by pulmonary mononuclear cells of F344/N-rnu nude rats was relatively higher than that of CD4. In F344 rats, CD8 expression increased gradually, reached a peak 6 weeks after infection, and then decreased gradually (Fig. 4A). The CD4/CD8 ratio in the infected lung tissues was always less than 1.0 at any point after infection. Anti-CD8 monoclonal Ab (Serotec) was also reactive with immature T-cells. MCA1427 antigen (NK cells) expression was highest 1 week after infection and then decreased gradually. A similar expression pattern was also recognized for α/β T-cell expression, which reached a peak 1 week after infection, but decreased 3 weeks after infection. There were relatively few γ/δ T-cells among the pulmonary mononuclear cells obtained from F344/N-rnu nude rats (less than 2%). In F344 rats, their number increased 6 weeks after infection, but decreased 12 weeks after infection (Fig. 4B).

Discussion

We have shown that F344/N-rnu nude rat tuberculosis is similar to the tuberculosis observed in immunocompromised humans (i.e. that associated with HIV infection or the elderly), whereas that in F344 wild-type rats is similar to murine tuberculosis in that the granulomas lack central necrosis. The pulmonary granulomas in F344/N-rnu nude rats showed central necrosis and were surrounded by thick collagen fibres, but unlike those in humans, the central necrosis was not caseous. We have previously succeeded in inducing such granulomas with central necrosis in IFN-γ-deficient mice (Sugawara *et al.*, 1998). When IFN-γ-deficient mice were infected with the relatively avirulent BCG Pasteur, they developed multiple granulomas with central necrosis and multinucleated giant cells (Sugawara *et al.*, 1998). There was no evidence of macrophages surviving in the necrotic lesions when bacterial loads had reached very high levels. This finding was confirmed by the absence of Mac-3-positive macrophages in or near the necrotic lesions in IFN-γ knockout mice, but epithelioid macrophages were present in the necrotic lesions of F344/N-rnu nude rats. We have also shown that multinucleated giant cells are of alveolar macrophage origin. Therefore, it is speculated that marked reduction of IFN-γ is closely associated with the formation of granulomas with central necrosis. Studies of this nude rat model may have relevance to tuberculosis in AIDS patients and the elderly. As CD4 function declines in HIV infection, IFN-γ production by helper T-cells is reduced. The pattern of *M. tuberculosis* infection in AIDS patients is frequently more diffuse than that seen in classical tuberculosis, but is characterized by extensive tissue necrosis. A similar pattern of infection is also recognized in elderly patients with tuberculosis who are immunocompromised.

The F344/N-rnu nude rats we used are derived from the Rowett nude rat strain established in 1975. Since then, the nude rats have been maintained at Japan CLEA, Tokyo, and are commercially available. When we performed necropsy of uninfected F344/N-rnu nude rats, we found remnant thymus tissue in adipose tissue, but relative loss of T-cells was noted in the interfollicular area. If the original Rowett nude rat is characterized by hair loss and complete absence of the thymus, then the F344/N-rnu nude rat differs slightly from the parent strain. Although the F344/N-rnu nude rat is not a complete nude rat, FACS analysis showed that the T-cell population was decreased significantly. Immunologically therefore this rat strain is similar to humans with HIV infection whose T-cell population is decreased. *M. tuberculosis*-infected F344/N-rnu nude rats died of disseminated tuberculosis,

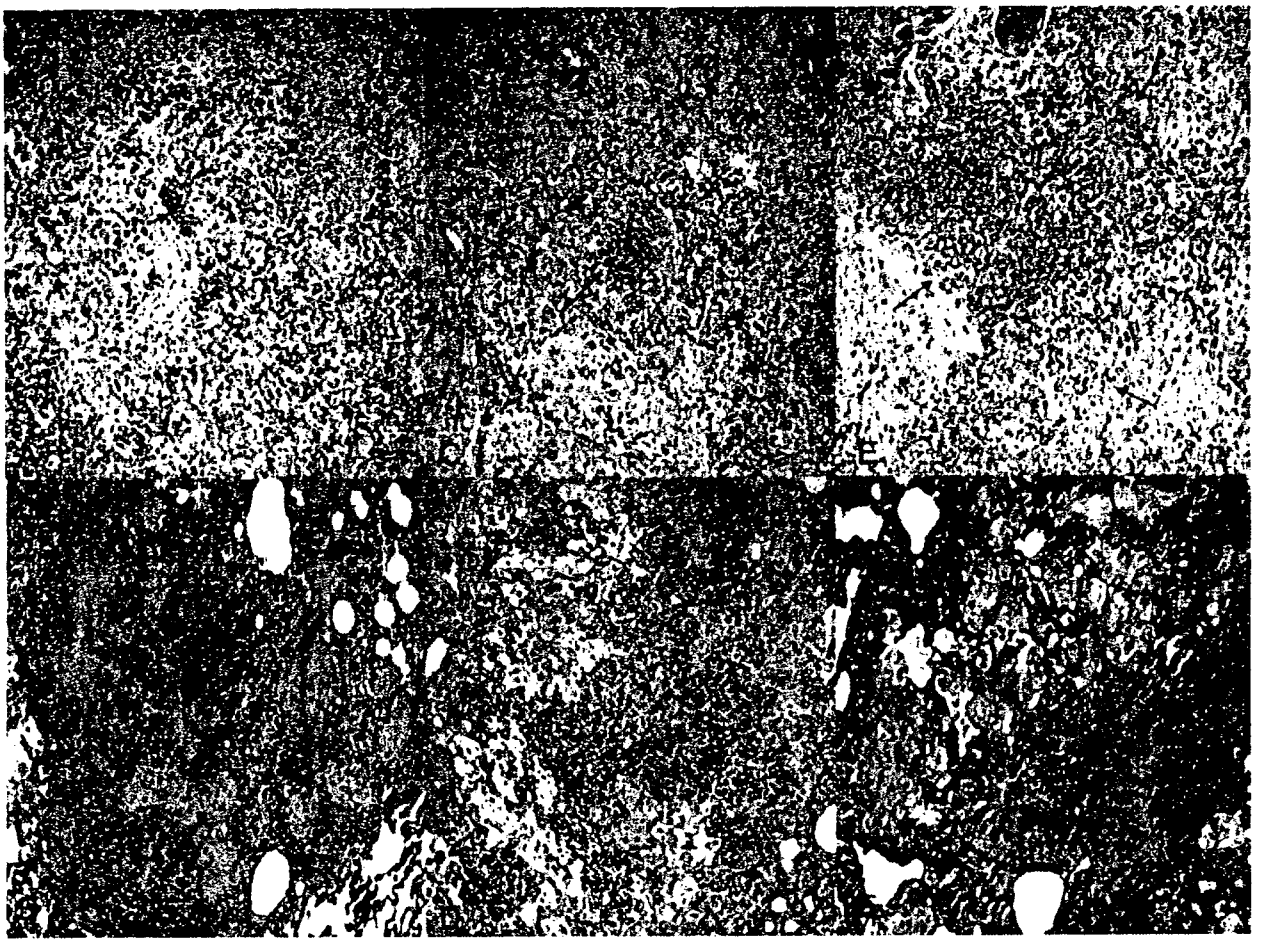

Fig. 3. Histological examination of lung tissues. Rats were sacrificed 3, 8 and 12 weeks after aerosol infection with the Kurono strain, and formalin-fixed sections were stained with HE. ×100.
A. Pulmonary tissue from a nude rat 3 weeks after infection with the Kurono strain. Arrow ((ρ)) indicates small necrotic lesion.
B. Pulmonary tissue from an F344 wild-type rat 3 weeks after infection with the Kurono strain. ×100.
C. Pulmonary tissue from a nude rat 8 weeks after infection with the Kurono strain. ×100. Central necrosis ((ρ)) is more prominent.
D. Pulmonary tissue from an F344 wild-type rat 8 weeks after infection with the Kurono strain.
E. Pulmonary tissue from nude rat 12 weeks after infection with the Kurono strain. Several necrotic lesions ((ρ)) are present.
F. Pulmonary tissue from an F344 wild-type rat 12 weeks after infection with the Kurono strain. Foamy macrophages are present in clusters, but no necrosis is noted in (B), (D) and (F).

whereas *M. tuberculosis*-infected F344 wild-type rats survived. There are few reports on FACS analysis of cell populations in nude rats, and this is one of the reasons why FACS was utilized in the present study. FACS analysis also showed that anti-CD4 and anti-CD8 monoclonal Abs (both Serotec) were significantly reactive with T-cells from the spleen. T-cells positive for OX52 antigen (equivalent to CD6), CD4 and CD8 were present in the infected lung tissues of the F344/N-rnu nude rats, but they remained at the same level throughout the course of infection. OX62-positive cells (dendritic cells and macrophages) in the infected lung tissues were fewer than those in F344 rats. Although this anti-OX62 monoclonal Ab reacts with macrophages, it is also a marker of dendritic cells (Sugawara *et al.*, 2004a). There were many ED1-positive macrophages in the infected lung tissues of both F344 and F344/N-rnu nude rats and there was no significant difference in percentage positivity between the two strains. This is also consistent with data showing that ED-1-positive cells are abundant in Lewis rat tuberculosis (Sugawara *et al.*, 2004a). Although there were significant numbers of NK cells in the *M. tuberculosis*-infected lung tissues, there was no significant difference in NK cell number between F344 and F344/N-rnu nude rats. α/β T-cells participate in acquired resistance to intracellular bacteria. In this study, the number of α/β T-cells was significantly lower in F344/N-rnu nude rats than in F344 rats, and there were fewer γ/δ T-cells in the infected lung tissues than in Lewis rats (Sugawara *et al.*, 2004a). At present, the reason for this is unclear, and further study

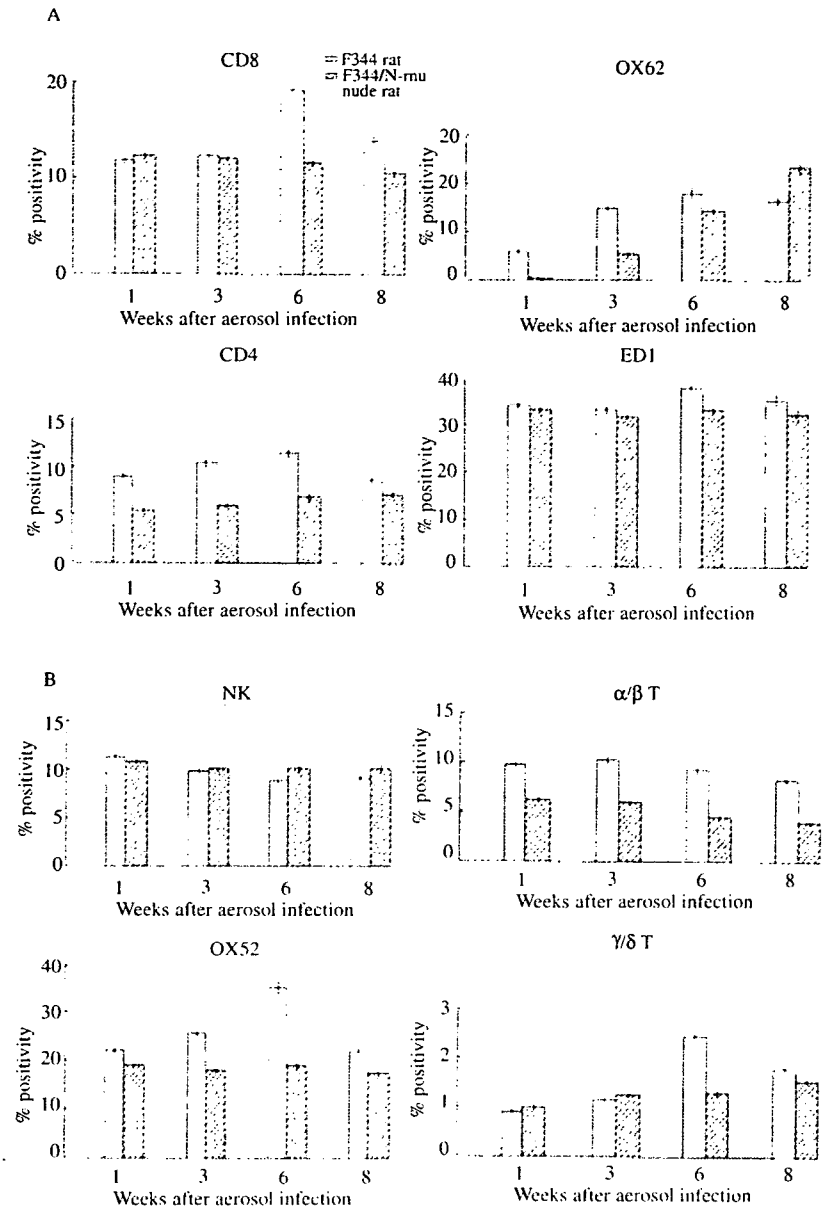

Fig. 4. Fluorescence-activated cell sorter (FACS) profiles of CD4-, CD8-, OX52 antigen-, OX62 antigen-, ED1 antigen-expressing mononuclear cells, NK cells, αβ T-cells, and γδ T-cells in mononuclear cells obtained from *M. tuberculosis*-infected rat lung tissue. (A) CD4, CD8, ED1 and OX62 antigen expression, and (B) NK cell, OX52 antigen, αβ T-cell and γδ T-cell expression.

will be required to confirm that γ/δ T-cells actively participate in antibacterial immunity.

IFN-γ is an absolute requirement for activation of alveolar macrophages, and IL-2 is needed for activation of Th1 cells that secrete IFN-γ. iNOS is responsible for production of nitric oxide (NO), which is one of the agents involved in *M. tuberculosis* killing. Therefore, relative loss of these molecules allows proliferation of tuberculosis in nude rats, ultimately leading to death due to disseminated disease. By analogy, expression of IFN-γ, IL-2 and iNOS mRNA may be low when granulomas in human tuberculosis develop central necrosis (Jitsukawa *et al.*, 1987; Sugawara *et al.*, 2003).

In summary, our nude rat tuberculosis model is similar to the tuberculosis seen in immunocompromised humans. Furthermore, it is easy to obtain mononuclear cells from lung tissues of *M. tuberculosis*-infected rats for immunological study and the animals are suitable for the tuberculin test. These features make the model ideal for immunological studies of tuberculosis *in vivo*.

Experimental procedures

Rats

Eight-week-old female F344 rats and F344/N-rnu nude rats were purchased from Japan CLEA, Tokyo, Japan. Necropsy revealed

that the F344/N-rnu nude rats had remnant thymus tissue, in which 24.09 ± 1.1% and 29.76 ± 1.4% of the T-cells were reactive with anti-CD4 (Serotec) and anti-CD8 (Serotec) Abs respectively. All the rats were housed in a biosafety level 3 facility and were given rat chow and water *ad libitum* after aerosol infection with virulent mycobacteria.

Antibodies

The following monoclonal Abs were used in this study: OX8 (anti-rat CD8 monoclonal Ab; Serotec), OX52 (anti-T lymphocyte monoclonal Ab; Serotec), OX52 (anti-rat T-cell monoclonal Ab; Serotec), OX62 (anti-rat dendritic cell monoclonal Ab; Serotec), anti-rat CD4 monoclonal Ab (Serotec) and ED1 (anti-rat dendritic cell/macrophage/monocyte monoclonal Ab; Serotec). Fluorescein isothiocyanate (FITC)-conjugated OX52m phycoerythrin (PE)-conjugated OX62, FITC-conjugated ED1, -OX8, -anti-rat CD4 monoclonal Ab, and -MCA1427 anti-rat NK cell monoclonal Ab; Serotec) were purchased from Dainippon Seiyaku, Osaka, Japan (Brideau *et al.*, 1980; Robinson *et al.*, 1986; Brenan and Puklavec, 1992; Vidal *et al.*, 1993; Damoiseaux *et al.*, 1994; Sedgwick, 1998) and FITC-conjugated anti-rat α/β T-cell monoclonal Ab (BD Biosciences) and FITC-conjugated anti-rat γ/δ T-cell monoclonal Ab (BD Biosciences) were purchased from Fujisawa Pharmaceutical, Tokyo, Japan (Paterson *et al.*, 1987; Kuhnlein *et al.*, 1994).

Experimental infection

A virulent strain (Kurono) of *M. tuberculosis* (ATCC 35812) was grown in Middlebrook 7H9 broth for 2 weeks, and then filtered through a sterile acrodisc syringe filter (Pall, Ann Arbor, MI, USA) with a pore size of 5.0 μm. Aliquots of the bacterial filtrate were stored at −80°C until use. F344 rats and F344/N-rnu nude rats were infected via the airborne route by placing them in the exposure chamber of a Glas-Col aerosol generator (Glas-Col, Terre Haute, IN). The nebulizer compartment was filled with 5 ml of a suspension containing 1×10^6 cfu of Kurono tubercle bacilli so that less than 100 bacteria would be deposited in the lung of each animal (Whiteland, 1995; Sugawara *et al.*, 1999; Yamada *et al.*, 2001).

Mycobacterial enumeration

At 1, 3, 6, 8 and 12 weeks after aerial infection, the rats were anaesthetized with pentobarbital sodium, the abdominal cavity was opened, and exsanguination was performed by splenectomy. The lungs, spleen and liver were excised and weighed. The left lung and part of the spleen were weighed separately and used to evaluate *in vivo* growth of mycobacteria. The lung and spleen tissues were homogenized with a mortar and pestle, and 1 ml of sterile saline was then added. One hundred microlitres of homogenate was then plated in a 10-fold serial dilution series on 1% Ogawa egg medium. Colonies were counted after 4 weeks of incubation at 37°C (Whiteland, 1995; Sugawara *et al.*, 2001).

Histopathology

For light microscopic examination, the right lung was excised and fixed with 20% formalin-buffered methanol solution (Mildform 20 NM, containing 8% formaldehyde and 20% methanol; Wako Pure Chemical, Osaka, Japan), dehydrated in a graded ethanol series, treated with xylene, and embedded in paraffin. Sections (5 μm) were cut from each paraffin block and stained with HE, Masson's trichrome for collagen fibres or Ziehl-Neelsen stain for acid-fast bacilli.

Fluorescence-activated cell sorter (FACS) analysis

Pulmonary mononuclear cells were isolated by homogenizing the *M. tuberculosis*-infected lung tissue carefully and evenly with a homogenizer and washing three times with phosphate-buffered saline (PBS). After blocking with 5% bovine serum albumin, the cells were stained with PE-conjugated OX62, FITC-conjugated ED1, -OX8, -OX52, -anti-rat CD4 monoclonal Ab, -MCA1427, -α/β T-cell monoclonal Ab, and -γ/δ T-cell monoclonal Ab for 20 min at 4°C. Thereafter, the cells were fixed in 2% paraformaldehyde/PBS, examined with a FACS (FACSCAN, BD) (Sugawara *et al.*, 2004a) and analysed with Cell Quest software (Pharmingen). For ED1 immunostaining, the mononuclear cells were made permeable with 0.1% saponin for 15 min before reaction with ED1.

Statistical analysis

All values are expressed as means ± SE, and were compared using Student's *t*-test. For all statistical analyses, differences at $P < 0.01$ were considered to be statistically significant.

Acknowledgements

This study was supported in part by an International Collaborative Study Grant to the chief investigator, Dr Isamu Sugawara, from the Ministry of Health, Labor and Welfare, Japan.

References

Aung, H., Toossi, Z., McKenna, S.M., Gogate, P., Sierra, J., Sada, E., and Rich, E.A. (2000) Expression of transforming growth factor-β but not tumor necrosis factor-α, interferon-γ, and interleukin-4 in granulomatous lung lesions in tuberculosis. *Tuberc Lung Dis* **80:** 61–67.

Banyai, A.L. (1931) Diabetes and pulmonary tuberculosis. *Am Rev Tuberc* **24:** 650–667.

Boucot, K., Dillon, E., Cooper, D., and Muer, P. (1952) Tuberculosis and diabetics. *Am Rev Tuberc* **65** (Suppl. 1): 1–50.

Brenan, M., and Puklavec, M. (1992) The MRC OX-62 antigen: a useful marker in the purification of rat veiled cells with the biochemical properties of an integrin. *J Exp Med* **175:** 1457–1465.

Brideau, R.J., Carter, P.B., Mcmaster, W.R., Mason, D.W., and Williams, A.F. (1980) Two subsets of rat T lymphocytes defined with monoclonal antibodies. *Eur J Immunol* **10:** 609–615.

Damoiseaux, J.G., Dopp, E.A., Calame, W., Chao, D., MacPherson, G.G., and Dijkstra, C.D. (1994) Rat macrophage lysosomal membrane antigen recognized by monoclonal antibody ED1. *Immunology* **83:** 140–147.

Dannenberg, A.M., Jr. (1999) Pathobiology: basic aspects. In *Tuberculosis and Nontuberculous Mycobacterial Infections.* Schlossberg, D. (ed.). Philadelphia, PA: W.B. Saunders, pp. 17–28.

Francis, J. (1958) *Tuberculosis in Animals and Man. A Study in Comparative Pathology*. London: Cassell & Company, pp. 237–242.

Jitsukawa, T., Nakajima, S., and Sugawara, I. (1987) Characterization of murine monoclonal antibodies to human IFN-γ and their application for sandwich ELISA. *Microbiol Immunol* **32:** 809–820.

Kuhnlein, P., Park, J.H., Herrmann, T., Elbe, A., and Hunig, T. (1994) Identification and characterization of rat γδ T lymphocytes in peripheral lymphoid organs, small intestine, and skin with a monoclonal antibody to a constant determinant of the γδ T cell receptor. *J Immunol* **153:** 979–986.

Kuramoto, T., Serikawa, T., Hayasaka, N., Mori, M., and Yamada, J. (1993) Regional mapping of the Rowett nude gene (RONU) to rat chromosome 10q24–>q32 by localizing linked SYB2 and GH loci. *Cytogenet Cell Genet* **63:** 107–110.

McMurray, D.N. (1994) Guinea pig model of tuberculosis. In *Tuberculosis: Pathogenesis, Protection, and Control*. Bloom, B.R. (ed.). Washington, DC: American Society for Microbiology Press, pp. 135–148.

Orme, I.M., and Collins, F.M. (1994) Mouse model of tuberculosis. In *Tuberculosis: Pathogenesis, Protection, and Control*. Bloom, B.R. (ed.). Washington, DC: American Society for Microbiology Press, pp. 113–134.

Paterson, D.J., Jefferies, W.A., Green, J.R., Brandon, M.R., Corthesy, P., Puklavec, M., and Williams, A.F. (1987) Antigens of activated T lymphocytes including a molecule of 50 000 Mr detected only on CD4 positive T blasts. *Mol Immunol* **24:** 1281–1290.

Robinson, A.P., Puklavec, M., and Mason, D.W. (1986) MRC OX-52: a rat T-cell antigen. *Immunology* **57:** 527–531.

Root, H.F. (1934) The association of diabetes and tuberculosis. *N Engl J Med* **210:** 1–13.

Scott, H.M., and Flynn, J. (2002) *Mycobacterium tuberculosis* in chemokine receptor 2-deficient mice: influence of dose on disease progression. *Infect Immun* **70:** 5946–5954.

Sedgwick, J.D. (1998) Central nervous system microglial cell activation and proliferation follows direct interaction with tissue-infiltrating T cell blasts. *J Immunol* **160:** 5320–5330.

Selva, E., Hofman, V., Berto, F., Musso, S., Castillo, L., Santini, J., *et al.* (2004) The value of polymerase chain reaction detection of *Mycobacterium tuberculosis* in granulomas isolated by laser capture microdissection. *Pathology* **36:** 77–81.

Sugawara, I., Yamada, H., Kazumi, Y., Doi, N., Otomo, K., Aoki, T., *et al.* (1998) Induction of granulomas in IFN-γ gene-disrupted mice by avirulent but not by virulent strains of *Mycobacterium tuberculosis*. *J Med Microbiol* **47:** 871–877.

Sugawara, I., Yamada, H., Kaneko, H., Mizuno, S., Takeda, K., and Akira, S. (1999) Role of IL-18 in mycobacterial infection in IL-18 gene-disrupted mice. *Infect Immun* **67:** 2585–2589.

Sugawara, I., Mizuno, S., Yamada, H., Matsumoto, M., and Akira, S. (2001) Disruption of NF-IL6, a transcription factor, results in severe mycobacterial infection. *Am J Pathol* **158:** 361–366.

Sugawara, I., Yamada, H., and Mizuno, S. (2003) Relative importance of STAT4 in murine tuberculosis. *J Med Microbiol* **52:** 29–34.

Sugawara, I., Yamada, H., and Mizuno, S. (2004a) Pathological and immunological profiles of rat tuberculosis. *Int J Exp Pathol* **85:** 125–134.

Sugawara, I., Yamada, H., and Mizuno, S. (2004b) Pulmonary tuberculosis in spontaneously diabetic Goto Kakizaki rats. *Tohoku J Exp Med* **204:** 135–145.

Vidal, S.M., Malo, D., Vogan, K., Skamene, E., and Gros, P. (1993) Natural resistance to infection with intracellular parasites: isolation of a candidate for Bcg. *Cell* **73:** 469–485.

Wessels, C.C. (1941a) Tuberculosis in the rat. I. Gross organ changes and tuberculin sensitivity in rats infected with tubercle bacilli. *Am Rev Tuberc* **43:** 449–458.

Wessels, C.C. (1941b) Tuberculosis in the rat. III. The correlation between the histological changes and the fate of living tubercle bacilli in the organs of the Albino rat. *Am Rev Tuberc* **43:** 637–662.

Whiteland, J.L. (1995) Immunohistochemical detection of T cell subsets and other leukocytes in paraffin embedded rat and mouse tissues with monoclonal antibodies. *J Histochem Cytochem* **143:** 313–320.

Yamada, H., Mizuno, S., Reza-Gholizadeh, M., and Sugawara, I. (2001) Relative importance of NF-κB p50 in mycobacterial infection. *Infect Immun* **69:** 7100–7105.

INT J TUBERC LUNG DIS 9(9):1052–1053

SHORT COMMUNICATION

Low antibody response against tuberculous glycolipid (TBGL) in elderly gastrectomised tuberculosis patients

J. Ashino, Y. Ashino, H. Guio, H. Saitoh, M. Mizusawa, T. Hattori

Division of Infectious and Respiratory Diseases, Graduate School of Medicine, Tohoku University, Sendai, Japan

SUMMARY

To evaluate differences in anti-tuberculous glycolipid (TBGL) antibody titers in patients who developed tuberculosis (TB) with and without gastrectomy, 11 gastrectomised patients who developed TB after surgery (GS-TB), 19 TB patients without any other complications (TB), 12 gastrectomised patients who did not develop TB after surgery (GS) and 27 healthy subjects (H) with normal findings on chest X-ray were evaluated, although there were no differences in the clinical findings at admission between the TB and GS-TB groups. The assay used here allowed us to find low anti-TBGL antibody titers in GS-TB patients.

KEY WORDS: TBGL; gastrectomy; tuberculosis

GASTRECTOMY is known as an associated co-factor in the development of tuberculosis (TB). Although the reasons for the association have not been clarified,[1,2] previous studies with a significant number of gastrectomised patients have reported prevalences of 1.7% to 2.5%. In addition, immunodeficiency and/or malnutrition contribute to the development of TB.[3] We therefore evaluated the clinical and laboratory findings, including purified protein derivative (PPD) reaction, in TB and/or gastrectomised patients and healthy controls. In the gastrectomised patients, group 2 lymph nodes were dissected, which could have affected the host immune responses. The glycolipid antigen trehalose 6, 6′-dimycolate (TDM) purified from *Mycobacterium tuberculosis* H37Rv has recently been reported as a useful diagnostic antigen.[4–6] We thus investigated specific immune responses against TDM by measuring anti-tuberculous glycolipid (TBGL) antibody titers.

Between 1999 and 2001, a total of 60 patients from Tohoku University Hospital enrolled in the study were divided into four groups: 1) gastrectomised patients who developed TB after surgery (GS-TB, n = 11); 2) TB patients without any other complications (TB, n = 19); 3) gastrectomised patients who did not develop TB after surgery (GS, n = 12); and 4) healthy subjects (n = 27) with normal findings on chest X-ray. For both TB and GS-TB patients, blood samples were taken before anti-tuberculosis drugs were given.

The study was approved by the ethics committee of the Tohoku University School of Medicine. Informed consent was obtained from patients and volunteers to participate in the study. For the diagnosis of TB, in addition to clinical features, acid-fast smear, culture and polymerase chain reaction tests (Roche Amplicor Mycobacterium Kit, Branchburg, NJ, USA) were performed using sputum or gastric fluid. Gastrectomised patients with recurring cancer, those treated with anticancer drugs and those with other diseases were excluded. Immunoglobulin G (IgG) antibodies against TBGL antigen was measured using an enzyme-linked immunosorbent assay (ELISA) kit (Kyowa Medex Co, Tokyo, Japan). A cut-off value ≥2 U/ml was considered positive.[4,5] Statistical analyses were performed using conventional methods.

Mean age and postoperative duration were 74.5 ± 9.2 years and 24.3 ± 6.3 months in the GS-TB group and 74.8 ± 3.0 years and 20.6 ± 9.2 months in the GS group, respectively. There were no significant differences between the two groups ($P > 0.05$). The mean ages in the TB patients and healthy controls were respectively 73.0 ± 9.4 and 73.2 ± 8.2 years. There were no significant differences in positive tuberculin test (6/11 vs. 10/19), lung infiltration shadow (≥2 lobes) (5/11 vs. 14/19) or acid-fast smear (≥1/field) (6/11 vs. 10/19) between the GS-TB and TB groups.

In this study, 55% of the GS-TB patients were positive for the anti-TBGL antibody titers by ELISA; this result was comparable to that obtained for the TB patients (68%). Maekura et al. found a significant number (17%) of TBGL-positive serum samples in healthy individuals.[5] In our healthy subjects, 22% of serum samples showed positive responses, but curiously none of the GS group was positive. Furthermore, the anti-TBGL antibody titers in the GS-TB patients were

Correspondence to: Dr Toshio Hattori, Division of Infectious and Respiratory Diseases, Graduate School of Medicine, Tohoku University, 1-1 Seiryo-machi, Aoba-ku, Sendai 980-8574, Japan. Tel: (+81) 22 717-8220. Fax: (+81) 22 717-8221. e-mail: thattori@int1.med.tohoku.ac.jp

Article submitted 14 October 2004. Final version accepted 28 January 2005.

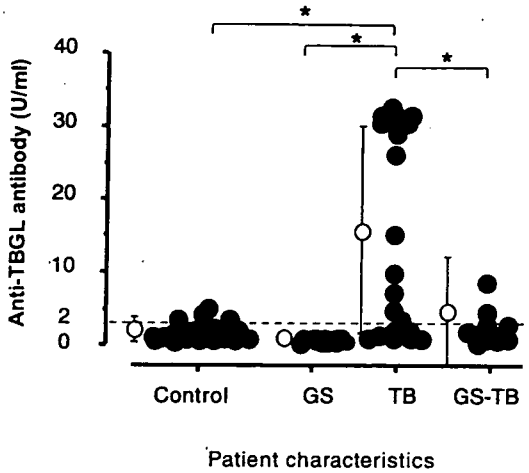

Figure 1 Individual anti-TBGL values in healthy controls and GS, TB and GS-TB patients. Circles = individual anti-TBGL values; bars = standard deviation; dotted line = cut-off; anti-TBGL = anti-tuberculous glycolipid; GS = gastrectomised; TB = tuberculosis. * $P < 0.05$.

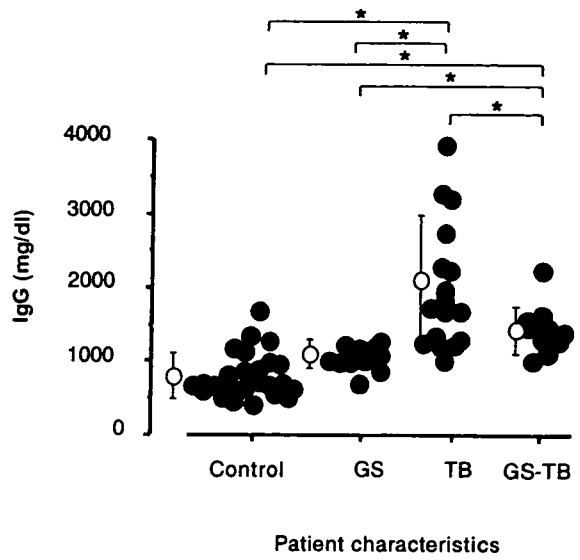

Figure 2 Individual IgG values in healthy controls and GS, TB and GS-TB patients. Circles = individual IgG values; bars = standard deviation; IgG = immunoglobulin G; GS = gastrectomised; TB = tuberculosis. * $P < 0.05$.

significantly lower than those of the TB patients ($P < 0.05$) (Figure 1). The serum IgG in both TB and GS-TB patients was significantly higher than in the GS patients and healthy controls (Figure 2), confirming that the decrease of anti-TBGL antibody in GS-TB patients could not be explained by the low IgG in their serum. It should also be noted that both anti-TBGL antibody and total IgG values were lower among GS-TB patients than in the TB group.

The reason for the lack of anti-TBGL antibody in GS patients and the low anti-TBGL antibody titers in GS-TB patients is not clear, but both suggest that the stomach may play a role in the production of anti-TBGL antibodies.

Acknowledgements

This work was supported by Grant-in-Aid for Scientific Research B and Exploratory Research from JSPS (Japan Society for the Promotion of Science), a Health Sciences Research Grant from the Ministry of Health, Labor and Welfare of Japan. We are grateful to Dr Sasaki and Dr Shiiba at the Division of Biological Regulation and Oncology in the Department of Surgery for supplying the serum from gastrectomised patients. We are also grateful to Dr Yano at Japan BCG Laboratory for critical reading of the manuscript.

References

1 Snider D E. Tuberculosis and gastrectomy. Chest 1985; 87: 414–415. [Editorial]
2 Steiger Z, Nickel W O, Shannon G J, Nedwicki E G, Higgins R F. Pulmonary tuberculosis after gastric resection. Am J Surg 1976; 131: 668–671.
3 Dai G, Phalen S, McMurray D. Nutritional modulation of host responses to mycobacteria. Front Biosci 1998; 3: e110–122. [Review]
4 Maekura R, Nakagawa M, Nakamura Y, et al. Clinical evaluation of rapid serodiagnosis of pulmonary tuberculosis by ELISA with cord factor (Trehalose—6, 6′-dimycolate) as antigen purified from *Mycobacterium tuberculosis*. Am Rev Respir Dis 1990; 148: 997–1001.
5 Maekura R, Okuda Y, Nakagawa M, et al. Clinical evaluation of anti-tuberculouos glycolipid immunoglobulin G antibody assay for rapid serodiagnosis of pulmonary tuberculosis. J Clin Microbiol 2001; 39: 3603–3608.
6 De Smet K A, Weston A, Brown I N, Young D B, Robertson B D. Three pathways for trehalose biosynthesis in mycobacteria. Microbiology 2000; 146: 199–208.

RÉSUMÉ

Afin d'évaluer les différences entre les titres d'anticorps glycolipides anti-tuberculeux (TBGL) chez des patients ayant développé TB avec ou sans gastrectomie, ont été évalués 11 patients gastrectomisés ayant développé une TB après chirurgie (GS-TB), 19 patients TB sans autre complication (TB), 12 patients gastrectomisés n'ayant pas développé de TB après chirurgie (GS), et 27 sujets sains (H) présentant des radiographies thoraciques normales, bien qu'il n'y a eu aucune différence dans les investigations cliniques à l'admission entre les groupes TB et GS-TB. L'essai utilisé nous a permis de trouver de faibles titres d'anticorps d'anti-TBGL chez les patients GS-TB.

RESUMEN

Para evaluar la diferencia de títulos de anticuerpos para un glicolípido antituberculoso (TBGL), en pacientes infectados con TB con y sin antecedente de gastrectomía, se evaluaron 11 pacientes gastrectomisados (GS-TB), 19 pacientes infectados con TB sin otra complicación (TB), 12 pacientes gastrectomisados que no desarrollaron TB (GS) y 27 sanos (H) con exámenes radiológicos normales. No hubo diferencias significativas entre los grupos TB y GS-TB al ingreso. Los resultados mostraron bajos títulos anti-TBGL en pacientes GS-TB.

THE JOURNAL OF BIOLOGICAL CHEMISTRY VOL. 280, NO. 50, pp. 41137–41145, December 16, 2005

Catalase Plays a Critical Role in the CSF-independent Survival of Human Macrophages via Regulation of the Expression of BCL-2 Family*

Received for publication, September 7, 2005, and in revised form, September 19, 2005 Published, JBC Papers in Press, October 4, 2005, DOI 10.1074/jbc.M509793200

Iwao Komuro[‡§], Tomoyoshi Yasuda[¶], Aikichi Iwamoto[§], and Kiyoko S. Akagawa[‡1]

From the Departments of [‡]Immunology and [¶]Parasitology, National Institute of Infectious Diseases, Toyama 1-23-1, Shinjuku-ku, Tokyo 162-8640 and [§]Division of Infectious Diseases, the Advanced Clinical Research Center, Institute of Medical Science, University of Tokyo, Shiroganedai 4-6-1, Minato-ku, Tokyo 108-8639, Japan

M-colony-stimulating factor (M-CSF)-induced monocyte-derived macrophages (M-MΦ) required continuous presence of M-CSF for their survival, and depletion of M-CSF from the culture induced apoptosis, whereas human alveolar macrophages (A-MΦ) and granulocyte-macrophage (GM)-CSF-induced monocyte-derived macrophages (GM-MΦ) survived even in the absence of CSF. The expression of BCL-2 was higher in M-MΦ, and M-CSF withdrawal down-regulated the expression. The expression of BCL-X_L was higher in A-MΦ and GM-MΦ, and the expression was CSF-independent. The expression of MCL-1 and BAX were not different between M-MΦ and GM-MΦ and were CSF-independent. Down-regulation of the expression of BCL-2 and BCL-X_L by RNA interference showed the important role of BCL-2 and BCL-X_L in the survival of M-MΦ and GM-MΦ, respectively. Human erythrocyte catalase (HEC) and conditioned medium obtained from GM-MΦ or A-MΦ cultured in the absence of GM-CSF prevented the M-MΦ from apoptosis and restored the expression of BCL-2. The activity of the conditioned medium was abrogated by pretreatment with anti-HEC antibody. Anti-HEC antibody also induced the apoptosis of M-MΦ cultured in the presence of M-CSF and GM-MΦ and A-MΦ cultured in the presence or absence of GM-CSF and down-regulated the expression of BCL-2 and BCL-X_L in these MΦs. GM-MΦ and A-MΦ, but not M-MΦ, can produce both extracellular catalase and cell-associated catalase in a CSF-independent manner. Intracellular glutathione levels were kept equivalent in these MΦs, both in the presence or absence of CSF. These results indicate a critical role of extracellular catalase in the survival of human macrophages via regulation of the expression of *BCL-2* family genes.

Human tissue macrophages (MΦ)[2] play important roles for homeostasis, and *in vivo* alveolar (A)-MΦ acquire a strong antioxidant phenotype that contributes to prevention of the oxidant burst in an aerobic environment and can survive for long periods (1). In a previous study, we reported that human A-MΦ and GM-CSF-induced monocyte-derived macrophages (GM-MΦ) are resistant to hydrogen peroxide (H_2O_2) via their high basal and inducible levels of catalase activity and that M-CSF-induced monocyte-derived macrophages (M-MΦ) are sensitive to low levels of H_2O_2 with low levels of catalase activity (2). GM-MΦ is phenotypically identical to A-MΦ, whereas M-MΦ closely resembles peritoneal MΦ in respect to morphology, cell surface antigen expression, and several biological functions (2–7). *In vivo* A-MΦ express BCL-2 family proteins such as BCL-2 and BCL-X_L that prevent H_2O_2-induced apoptosis via inhibition of caspase-3 or -9 activation and cytochrome *c* release from mitochondria (8–11). These findings suggest that a high level of catalase activity enables long survival of GM-MΦ and A-MΦ with positive regulation of BCL-2 family protein.

In this study, we found that M-MΦ absolutely require CSF for their survival and express high levels of *BCL-2* gene and protein in the presence of M-CSF. In contrast to M-MΦ, GM-MΦ and A-MΦ can survive in the absence of CSF via high levels of *BCL-X_L* gene and protein. We further examined the relation between catalase activity and distinct expression of BCL-2 family protein and make clear the roles of CSF in the regulation of catalase activity and BCL-2 family protein in human tissue macrophages under the influence of oxidative stress.

EXPERIMENTAL PROCEDURES

Preparation and Culture of Macrophages—Monocytes (Mo) were obtained from peripheral blood mononuclear cells of normal healthy volunteers using a magnetic cell separation system (MACS; Miltenyi Biotec, Bergisch Gladbach, Germany) with anti-CD14 monoclonal antibody-coated microbeads as described previously (7). $CD14^+$ Mo were cultured in RPMI 1640 medium (Nissui Seiyaku Co., Ltd., Tokyo, Japan), 3 mg/ml filtered glutamine (Sigma), 100 units/ml penicillin G potassium (Banyu Seiyaku Co., Ltd., Tokyo, Japan), 100 μg/ml streptomycin (Meiji Seika Co., Ltd., Tokyo, Japan), 10% autoclaved $NaHCO_3$, and 10% heat-inactivated fetal calf serum (Z. L. Bockneck Laboratories Inc., Ontario, Canada) with the following human recombinant cytokines at optimal concentrations: 5 ng/ml GM-CSF (Schering-Plough Japan, Osaka, Japan) or 50 ng/ml M-CSF (Morinaga Milk Industry Co., Ltd., Tokyo, Japan) at 37 °C in humidified 5% CO_2 for 7 days. During the culture, Mo differentiated to MΦ.

Human A-MΦ were obtained from healthy volunteers (non-smokers without diseases) by bronchial alveolar lavage method (2, 7). All volunteers gave informed consent to the use of their A-MΦ in part for this study.

Antisense Oligonucleotide (AS) Treatment—2′-*O*-methyl-modified oligoribonucleotide phosphorothioate 18-mer two CpG motifs targeted to the *BCL-2* initiation codon (G3139 (BCL AS): 5′-TCTCCCAGCGT-

* This study was supported in part by grants for Research on Health Sciences Focusing on Drug Innovation from the Japan Health Sciences Foundation and the Ministry of Health, Labor, and Welfare of Japan. The costs of publication of this article were defrayed in part by the payment of page charges. This article must therefore be hereby marked "*advertisement*" in accordance with 18 U.S.C. Section 1734 solely to indicate this fact.

[1] To whom correspondence should be addressed. Tel.: 81-3-5285-1111; Fax: 81-3-5285-1150; E-mail: akagawak@nih.go.jp.

[2] The abbreviations used are: MΦ, macrophage; M-MΦ, M-CSF-induced monocyte-derived MΦ; A-MΦ, alveolar MΦ; GM-MΦ, granulocyte-macophage-CSF induced monocyte-derived MΦ; CSF, colony-stimulating factor; HEC, human erythrocyte catalase; CM, conditioned medium; Mo, monocytes; GSH, glutathione; AS, antisense oligonucleotide; BCL AS (G3139), 2′-*O*-methyl-modified oligonucleotide phosphorothioate 18-mer two CpG motifs targeted to the *BCL-2* initiation codon; BCL MS (G4126), G3139 variant with single base mismatch at each CpG motif; 5′-BCL-X AS, 2′-*O*-methyl-modified oligonucleotide phosphorothioate 18-mer to the 5′-splice site of BCL-X_L; MS, missense; anti-Cat ab, anti-HEC antibody.

GCGCCAT-3'), G3139 variant with single base mismatch at each CpG motif (G4126 (BCL missense (MS)): 5'-TCTCCCAGCATGTGCCAT-3') (12) and 18-mer to the 5'-splice site of BCL-X_L (5'-BCL-X AS, ACCCAGCCGCCGUUCUCC) (13) and *MCL-1* AS (ISIS 20408, TTGGCTTTGTGTCCTTGGCG) (14) were synthesized by Proligo France SAS (Paris, France). Oligonucleotides with random sequences were used as negative controls. Cells were treated with oligonucleotides complexed with Lipofectin (5 mg/ml; Invitrogen) cationic lipid delivery agent according to the manufacturer's directions.

Assessment of Cell Number and Cell Viability—The number of adherent Mo and MΦ was determined by counting the liberated intact nuclei from lysed cells stained with 1% (w/v) cetyltrimethyl ammonium bromide (Cetavelone; Wako Pure Chemical Industries, Ltd., Osaka, Japan) in 0.1 M citric acid with 0.05% (w/v) naphthol blue black (Sigma). Cell viability was assessed by the trypan blue dye exclusion test.

Assessment of Apoptosis—DNA fragmentation was detected by immunohistochemical staining using the terminal deoxynucleotidyl-transferase-mediated dUTP-biotin nick end-labeling method (Apo-tag kit; Oncor Co.) or visualized as DNA ladder formation (5). Cells were preincubated with 1% H_2O_2 in phosphate-buffered saline for inactivation of endogenous peroxidase for 5 min at room temperature. Incorporation of digoxigenin-conjugated dUTP to the terminal 3'-OH of fragmented DNA by exogenous terminal deoxynucleotidyl transferase was carried out at 37 °C for 1 h. The reaction products were incubated with horseradish peroxidase-linked anti-digoxigenin antibody at 37 °C for 30 min and visualized with the substrate 3–3' diaminobenzidine plus 0.6% H_2O_2.

Cells were lysed with hypotonic lysis buffer (10 mM Tris-Cl (pH 7.4), 10 mM EDTA (pH 8.0), 0.5% Triton-X), and crude DNA was extracted from the lysed cells by incubation with 40 μg/ml RNase and 40 μg/ml proteinase K for 1 h at 37 °C. The DNA was precipitated with final 50% propanol at −20 °C overnight and washed with 70% (w/v) ethanol. Electrophoresis was performed in 2% agarose at 50 V, and the migrated DNA was visualized by ethidium bromide staining.

Transmission Electron Microscopy—Cells were fixed by immersion in a 2.5% glutaraldehyde-2% paraformaldehyde mixture (10), followed by 1% glutaraldehyde-0.5% tannic acid diluted in 0.1 M cacodylate buffer (Wako Pure Chemical Industries, Ltd.) at 4 °C for 2 h. Samples were post-fixed with 1% OsO_4 (osmium tetroxide; Wako) at 4 °C for 2 h and then embedded in epoxy resin (Epok 812; Okenshoji. Co., Ltd., Tokyo). Thin sections were cut using a LKB-8800 ultratome (LKB, Uppsala, Sweden) and observed using a transmission electron microscope (Hitachi H-7000) after staining with uranyl acetate (Serva Electrophoresis GmbH)-0.2% lead citrate buffer (Wako).

Neutralization of Conditioned Medium—Conditioned medium was obtained from MΦ cultured in medium alone for 48 h at 37 °C and incubated for 60 min at 37 °C with 10 μg/ml rabbit anti-human erythrocyte catalase (HEC) IgG (lot PTC 9301; Athens Research and Technology, Inc., Athens GA) or with normal rabbit IgG (Organon Teknika Co.) as a control.

Measurement of Catalase Activity—Intracellular and extracellular catalase activity was measured according to Aebi's modified method as described previously (2). Purified HEC (5×10^4 units/mg, lot 643793; Calbiochem-Nova Biochem) was used for conversion of the catalase activity in samples into real catalase activity, and the activity was expressed as milliunits/ml per 2.5×10^5 cells or units/mg protein. Protein was measured using a protein assay kit (Bio-Rad Laboratories).

Measurement of GSH Level—The total GSH level was determined using a BIOXYTECH S. A. kit. Briefly, the cells were lysed with 5% metaphosphoric acid, and the chromophore formation catalyzed at pH 13.4 was measured at 400 nm as described previously (15). The intracellular GSH level was expressed as pmol/mg protein.

Isolation of RNA and Northern Blot Analysis—Isolation of total RNA and Northern blot analysis were performed as described previously (5). Blots were hybridized with cDNA probes against human catalase (kindly donated by Dr. K. Onozaki, Faculty of Pharmaceutical Sciences, Nagoya City University) and β-actin (Sigma). All the probes were labeled using a multiprime DNA-labeling system with [α-^{32}P]dCTP (New England Nuclear Research Products, Boston, MA). The blots were analyzed using a Fuji BAS 2000 bioimage analyzer (Fuji Photo Film Co., Ltd., Tokyo).

Immunoblot Analysis—Immunoblot analysis was performed as described in our previous report (7). The membrane was incubated overnight at 4 °C with 1 mg/ml rabbit anti-HEC antibody (anti-Cat Ab; Athens Research and Technology, Inc.), mouse anti-BCL-2 antibody (Santa Cruz Biotechnology, Santa Cruz, CA), rabbit anti-BCL-xL/S antibody (Santa Cruz Biotechnology), rabbit anti-BCL-X antibody (Transduction Laboratories, Lexington, KY), mouse anti-MCL-1 antibody (Santa Cruz Biotechnology), rabbit anti-BAX antibody (Santa Cruz Biotechnology), or normal rabbit or mouse IgG and then at room temperature for 1 h with horseradish peroxidase-conjugated goat anti-rabbit IgG or anti-mouse IgG (Santa Cruz Biotechnology). The blots were visualized with Amersham ECL reagent on Hyper ECL film (Amersham Biosciences).

Reverse Transcription and Polymerase Chain Reaction—Total RNAs (1 mg) were prepared by use of RNA Zol B (Cinna/Biotecx Laboratories, Friendswood, TX) and reverse transcribed by incubation in 50 μl of 10 mM Tris-HCl (pH 8.3), 6.5 mM $MgCl_2$, 50 mM KCl, 10 mM dithiothreitol, each dNTP at 1 mM, 2 mM random primer, and 2.4 units/ml Moloney murine leukemia virus reverse transcriptase for 1 h at 42 °C (Takara Shyzo, Otsu, Japan). The conditions for PCR were as follows: in a 50-μl reaction, 0.15 mM each primer, each dNTP at 2.5 mM, 50 mM KCl, 10 mM Tris-HCl (pH 8.3), 1.5 mM $MgCl_2$, and 1.25 units of *Taq* polymerase (Takara Shyzo). Primers used were as follows: glyceraldehyde-3-phosphate dehydrogenase: sense, 5'-CCTTCATTGACCTCAACTAC-3' and antisense, 5'-AGTGATGGCATGGACTGTGGT-3'; *BCL-2*: sense, 5'-CATTTCCACGTCAACAGAATTG-3' and antisense, 5'-AGCACAGGATTGGATATTCCAT-3'; *BCL-X_L*: sense, 5'-TTGGACAATGGACTGGTTGA-3' and antisense, 5'-GTAGAGTGGATGGTCAGTG-3'; *MCL-1*: sense, 5'-GAGGAGGAGGACGAGTTGTA-3' and antisense, 5'-CAGCTTTCTTGGTTTATGGT-3'; *BAX*: sense, 5'-AAGAAGCTGAGCGAGTGTC-3' and antisense, 5'-CGGCCCCAGTTGAAGTTGC-3'. Reactions were incubated in a PerkinElmer DNA thermal cycler for 25 cycles (with each cycle consisting of denaturation for 30 s at 95 °C, annealing for 30 s at 60 °C, and extension for 60 s at 72 °C) (5).

Statistical Analyses—Statistical analyses of the data were performed using Student's *t*-test. p values <0.01 were considered significant. The results shown are representative of three to seven independent experiments.

RESULTS

Requirement for Continuous Presence of CSF for the Survival of M-MΦ, but not of GM-MΦ and A-MΦ—M-MΦ, GM-MΦ, and A-MΦ were cultured with or without CSF, and then cell viability was determined. M-CSF withdrawal from M-MΦ induced cell death in a time-dependent manner; ~60% of the cells died by 2 days and almost all of the cells died by 8 days (Fig. 1*A*). In contrast, GM-CSF withdrawal from GM-MΦ or A-MΦ did not induce cell death significantly during the culture period (Fig. 1*A*). M-MΦ cultured in the absence of M-CSF

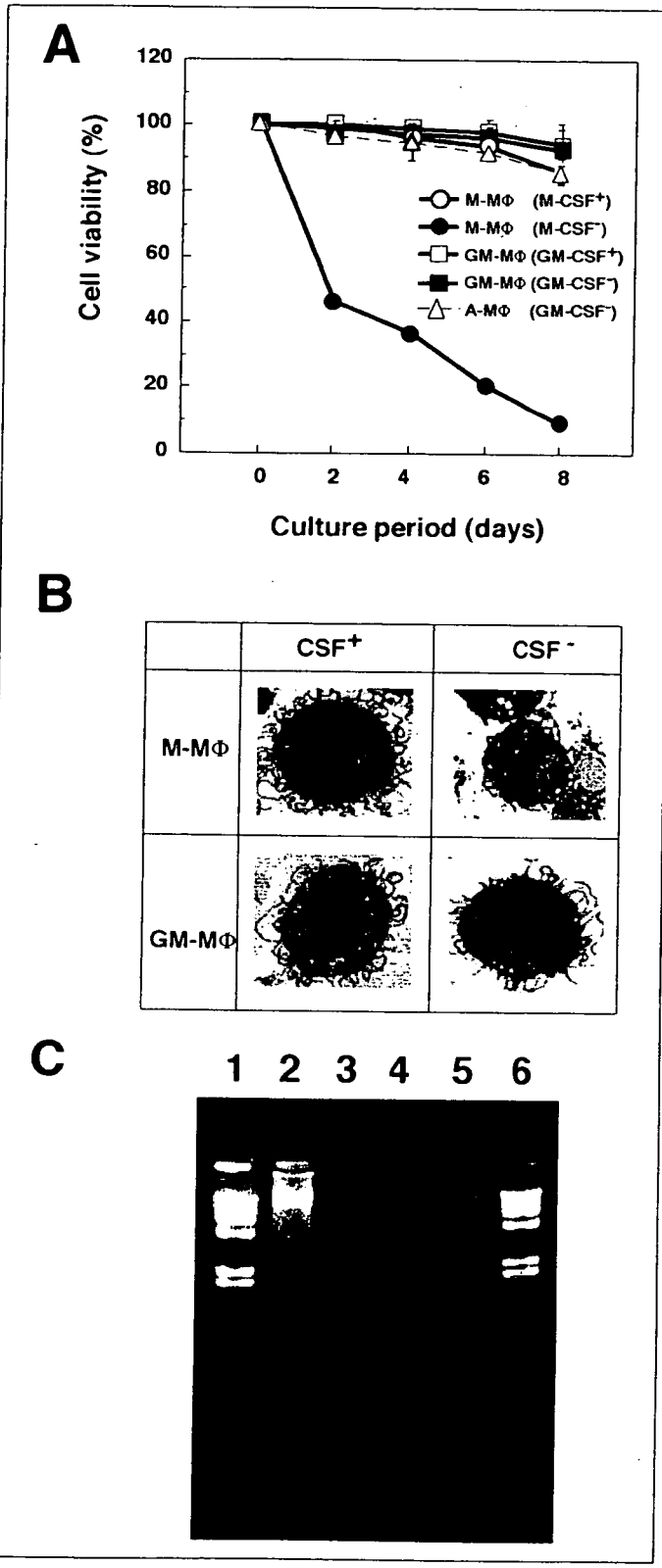

FIGURE 1. **Susceptibility of CSF-induced monocyte-derived MΦ and A-MΦ to CSF withdrawal.** M-MΦ and GM-MΦ (2.5×10^5/ml/well) were cultured in medium with or without M-CSF or GM-CSF, and A-MΦ were cultured in medium without GM-CSF. *A*, cell number and viability of MΦs were assessed using Cetavlon and trypan blue dye as described under "Experimental Procedures." Values are expressed as the means of triplicate cultures ± S.D. *B*, electron microscopic features of MΦ cultured in medium with or without CSF for 24 h (magnification ×10,000). *C*, electrophoresis of low molecular mass DNA from cultured MΦ. MΦ were incubated with M-CSF, GM-CSF, or medium alone for 24 h. Low molecular mass DNA was isolated from the cells, and electrophoresis was performed as described under "Experimental Procedures." HaeIII-digested I DNA fragment size standards were run in *lanes 1* and *6*. *Lane 2*, M-MΦ without M-CSF; *lane 3*, M-MΦ with M-CSF; *lane 4*, GM-MΦ without GM-CSF; *lane 5*, GM-MΦ with GM-CSF.

changed from spindle shaped to round and then detached from the dish and floated, with a shrunken cytosol and nucleus and with chromatin condensation and apoptotic vacuoles without microvilli (Fig. 1*B*). No such morphological change was observed in M-MΦ cultured with M-CSF or in GM-MΦ cultured with or without GM-CSF (Fig. 1*B*). A typical ladder pattern of internucleosomal DNA cleavage was detected in DNA of M-MΦ cultured for 24 h in the absence of M-CSF, whereas no significant DNA fragmentation was detected in DNA of M-MΦ cultured in the presence of M-CSF or that of GM-MΦ cultured in the presence or absence of GM-CSF (Fig. 1*C*). Apoptosis and DNA fragmentation of A-MΦ were similar to those of GM-MΦ (data not shown). These findings suggest that M-CSF withdrawal from M-MΦ induces apoptosis but both GM-MΦ and A-MΦ can survive in the absence of CSF.

Different Expression of BCL-2 and BCL-X_L Genes in M-MΦ, GM-MΦ, and A-MΦ and the Opposite Effect of CSF on Expression—*BCL-2* family genes play important roles in the apoptosis of many types of cells (10, 16–20). We therefore examined the expression of *BCL-2* family genes and the effect of CSF on their expression in M-MΦ and GM-MΦ by RT-PCR. In M-MΦ, the transcript of the *BCL-2* gene was stronger than that of the *BCL-X_L* gene, and M-CSF withdrawal decreased the expression of the *BCL-2* gene but induced a slight decrease in the expression of the *BCL-X_L* gene (Fig. 2*A*). In contrast to M-MΦ, GM-MΦ expressed strongly the *BCL-X_L* gene but weakly the *BCL-2* gene, and GM-CSF withdrawal had no significant effect on the expression of these two genes (Fig. 2*A*). In contrast to *BCL-2* and *BCL-X_L*, the transcriptional levels of the *MCL-1* and *BAX* genes were not significantly different between M-MΦ and GM-MΦ and were not affected by CSF deprivation (Fig. 2*A*). In accordance with the gene expression, the expression of the BCL-2 protein was higher in M-MΦ compared with GM-MΦ and M-CSF withdrawal decreased the expression of BCL-2 protein in M-MΦ (Fig. 2*B*). Similarly, the expression of the BCL-X_L protein was higher in GM-MΦ than in M-MΦ, but GM-CSF withdrawal had no significant effect on the expression of BCL-X_L protein in GM-MΦ (Fig. 2*B*).

The expression of BCL-2 family proteins in A-MΦ resembles that of GM-MΦ, and the expression was independent of CSF (Fig. 2*B*). As shown in Figs. 6 and 7, the expression of MCL-1 and BAX proteins in both MΦs was not changed in the presence or absence of CSF, in accordance with the expression patterns of the *MCL-1* and *BAX* genes.

HEC Stimulates the Survival and the Expression of BCL-2 in CSF-withdrawn M-MΦ, and Anti-HEC Antibody Abolishes the Survival-stimulating Activity of CM Obtained from CSF-withdrawn GM-MΦ and A-MΦ—The above findings suggest that GM-MΦ and A-MΦ, but not M-MΦ, can produce factor(s) that maintain their survival in the absence of CSF. To investigate this possibility, the conditioned medium (CM) obtained from these MΦ cultured for 48 h without CSF was used to examine its effect on the survival of M-CSF-withdrawn M-MΦ. CM of GM-MΦ or A-MΦ, but not of M-MΦ, prevented cell death of M-CSF-depleted M-MΦ (Fig. 3*A*).

A previous study showed that human CEM T cells can survive in serum-free medium supplemented with a low level of extracellular catalase (21). Therefore, we examined whether extracellular catalase prevents apoptosis in M-CSF-withdrawn M-MΦ and stimulates the expression of both *BCL-2* gene and protein. Addition of HEC prevented M-CSF-withdrawn M-MΦ from undergoing cell death in a dose-dependent manner, and 10 units/ml of HEC completely rescued the cells

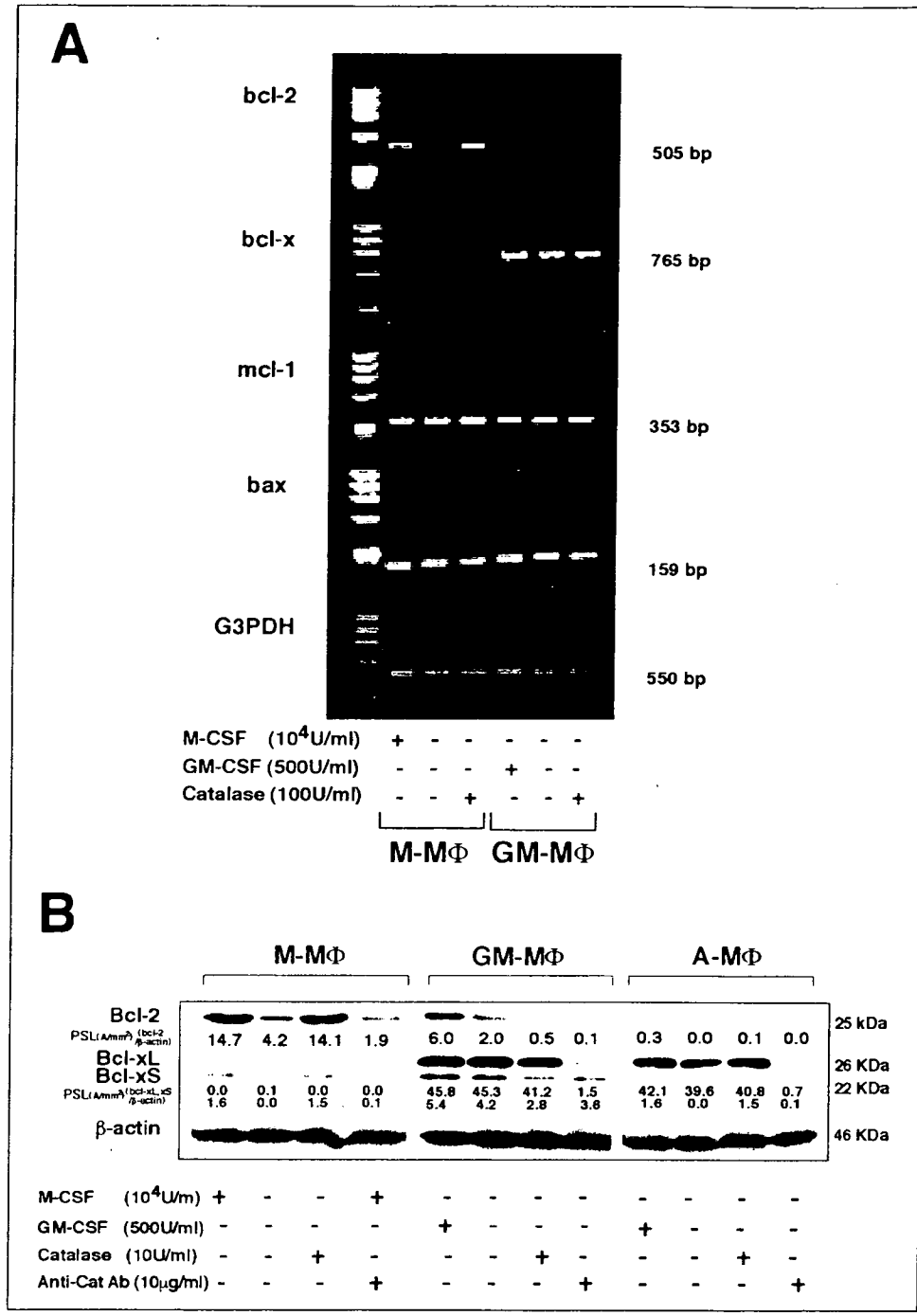

FIGURE 2. **Effects of CSF and catalase on the levels of protein and mRNA expression of *BCL-2* family genes in monocyte-derived MΦ and A-MΦ.** *A*, RT-PCR analysis of mRNA levels of *BCL-2* family genes and the glyceraldehyde-3-phosphate dehydrogenase gene in total RNA preparations (200 ng/lane) from these MΦs at 3 h of cultivation as described under "Experimental Procedures." M-MΦ and GM-MΦ were cultured in medium with or without CSF or supplemented with catalase. *B*, Western blot analysis of BCL-2, BCL-$X_L/_S$, or β-actin protein in cell lysates (25 μg/lane) probed using rabbit polyclonal BCL-2 or BCL-X antibody or mouse monoclonal β-actin antibody. M-MΦ were cultured for 48 h in medium with M-CSF or catalase or with M-CSF supplemented with anti-catalase antibody (*Anti-Cat Ab*), and GM-MΦ and A-MΦ were cultured in medium with GM-CSF or catalase or supplemented with Anti-Cat Ab. The relative amounts of these proteins in cells were measured using NIH image software, and the expression levels were corrected relative to those of β-actin (photo-stimulating luminescence (*PSL*), A/mm²).

from apoptosis. Addition of 10 units/ml HEC to GM-CSF-withdrawn GM-MΦ had no such effect (Fig. 3*A*).

Then we examined the effect of anti-HEC antibody (anti-Cat Ab) on the activity of the CM of GM-MΦ. Pretreatment of the CM with anti-Cat Ab, but not with control IgG, completely abrogated the ability to rescue the cell death of M-CSF-withdrawn M-MΦ (Fig. 3*B*). Similar results were obtained in experiments using the CM of A-MΦ (data not shown).

Next, we examined the role of catalase in the expression of *BCL-2* family genes in M-CSF-withdrawn M-MΦ. Addition of catalase to M-CSF-withdrawn M-MΦ restored the expression of *BCL-2* but did not affect the gene expression of *BCL-X_L*, *MCL-1*, or *BAX* (Fig. 2*A*). Addition of catalase did not significantly change the gene and protein expression of *BCL-2* family genes in GM-CSF-withdrawn GM-MΦ (Fig. 2*A*). These results suggest that the active molecule in the CM of GM-MΦ and A-MΦ that can rescue the survival of M-CSF-withdrawn M-MΦ via restoration of *BCL-2* expression is catalase.

Anti-catalase Antibody Abolished the Expression of BCL-2 in M-MΦ Cultured with M-CSF and BCL-X_L in GM-MΦ or A-MΦ Cultured with or without GM-CSF and Induced Apoptosis of These MΦs—The above results indicate that catalase can stimulate the expression of *BCL-2* and rescue the survival of M-CSF-withdrawn M-MΦ. Therefore we next examined whether extracellular catalase also plays a critical role in the CSF-dependent survival of M-MΦ and in the survival of GM-MΦ and A-MΦ. Addition of anti-Cat Ab suppressed the expression of BCL-2 protein in M-MΦ cultured in the presence of M-CSF and of BCL-X_L

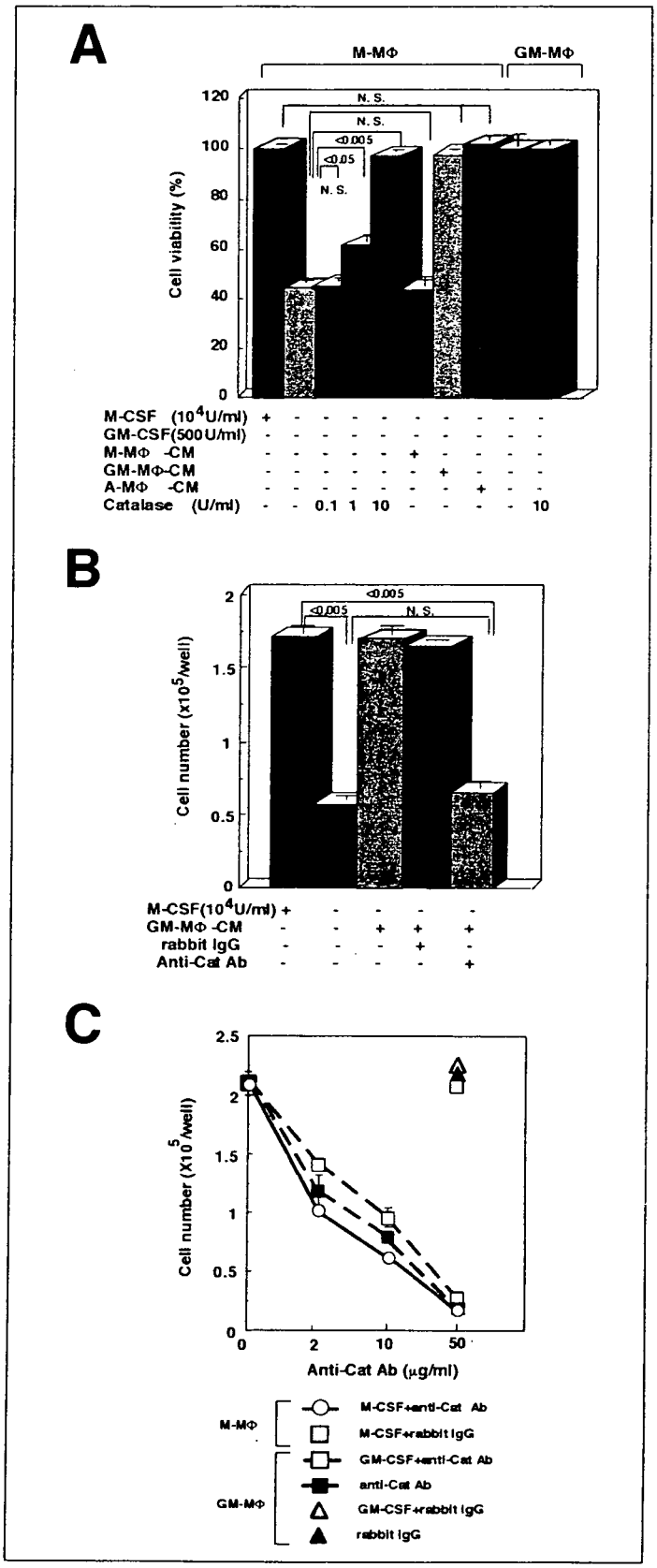

FIGURE 3. **Effect of endogenously produced or exogenously added catalase on the survival of M-MΦ and GM-MΦ.** *A*, M-MΦ were cultured for 48 h in the medium with M-CSF, medium containing the indicated concentrations of catalase, or 100% of conditioned medium (*CM*) obtained from M-MΦ, GM-MΦ, or A-MΦ. GM-MΦ were used as the control. Cell number and viability of MΦ were assessed as described in Fig. 1. Values are expressed as the means of triplicate cultures ± S.D. *B*, M-MΦ were cultured for 48 h in medium with M-CSF, CM pretreated with Anti-Cat Ab (*IgG*), or rabbit IgG as a control. Cell number and viability of MΦ were assessed as described in Fig. 1. Values are expressed as the means of triplicate cultures ± S.D. *C*, M-MΦ and GM-MΦ were cultured for 48 h in medium with or without CSF plus Anti-Cat Ab or rabbit IgG. Cell number and viability of MΦ were assessed as described in Fig. 1. Values are expressed as the means of triplicate cultures ± S.D.

protein in both GM-MΦ and A-MΦ cultured without GM-CSF (Fig. 2*B*). In accordance with these data, addition of anti-Cat Ab induced cell death of M-MΦ cultured with M-CSF and GM-MΦ cultured with or without GM-CSF, and addition of control IgG had no effect on the cell viability of these MΦs (Fig. 3*C*). The cell death of these MΦ induced by anti-Cat Ab was due to apoptosis, as indicated by terminal deoxynucleotidyl transferase-mediated dUTP-biotin nick end-labeling staining (data not shown).

GM-MΦ and A-MΦ, but Not M-MΦ, Can Produce Enough Levels of Extracellular Catalase in the Absence of CSF—The above results suggest that GM-MΦ and A-MΦ, but not M-MΦ, can produce extracellular catalase in a CSF-independent manner and that the catalase supports the survival of those MΦs via maintenance of the expression of *BCL-2* family genes. To examine this possibility, we measured catalase enzyme activity and catalase protein levels in the CMs of M-MΦ, GM-MΦ, and A-MΦ cultured for 48 h in the presence or absence of CSF. The extracellular catalase activities in the CMs obtained from GM-MΦ and A-MΦ cultured both in the presence or absence of GM-CSF were not significantly different, and the levels were ~4-fold higher (~240 milliunits/ml/well) than that of M-CSF-treated M-MΦ (~60 milliunits/ml/well) (Fig. 4*A*). In contrast to GM-MΦ or A-MΦ, the extracellular catalase activity in CM of M-MΦ was dependent on CSF and that in CM of M-CSF-withdrawn M-MΦ was significantly lower than that in CM of M-CSF-treated M-MΦ, ~20 milliunits/ml/well (Fig. 4*A*). Western blot analysis of the extracellular catalase of CMs using anti-HEC antibody showed similar results to the data of the enzyme activity (Fig. 4*A*).

Next, we examined the cell-associated levels of catalase activity in these MΦs (Fig. 4*B*). The levels of catalase activity in GM-MΦ and A-MΦ lysates was ~5 units/mg protein both in the presence or absence of CSF, whereas that in M-MΦ in the presence of M-CSF was ~1 unit/mg. The catalase activity in M-CSF-withdrawn M-MΦ lysates (~250 milliunits/mg protein) was ~4-fold lower than that in M-CSF-treated M-MΦ lysates. In agreement with the measurements of enzyme activity, similar results were observed in Western blot analyses (Fig. 4*B*).

To further confirm the distinction between the regulation of extracellular and cell-associated catalase activity by CSF in M-MΦ *versus* GM-MΦ, we examined the levels of transcription of the catalase gene in these MΦs cultured with or without CSF (Fig. 4*C*). The level of the transcript of the catalase gene in M-CSF-withdrawn M-MΦ was ~3-fold lower than that in M-CSF-treated M-MΦ. In contrast, the level of the catalase transcript in GM-CSF-withdrawn GM-MΦ and A-MΦ was similar to that in GM-CSF-treated GM-MΦ and A-MΦ, and the level was 5-fold higher than that in M-CSF-treated M-MΦ.

Thus, the difference of total extracellular plus intracellular catalase activity and the difference in the levels of catalase gene expression between CSF-withdrawn M-MΦ and GM-MΦ reached ~15–20- and ~15-fold, respectively. The results indicate that extracellular catalase activity is regulated at the transcription levels by CSF-dependent M-MΦ but CSF-independent GM-MΦ and A-MΦ.

Thiol Derivatives Act as Additive Effectors That Rescue the Cell Death of MΦ—The above data suggest that extracellular catalase plays a major role in MΦ survival. However, several reports have demonstrated that thiol proteins and thiol compounds such as GSH, adult T cell leukemia-derived factor, and L-cysteine play important roles in the survival of